C. R. Mecanique 347 (2019) 423–444

Contents lists available at ScienceDirect

Comptes Rendus Mecanique

www.sciencedirect.com

Data assimilation and pollution forecasting in Burgers' equation with model error function

Assimilation de données et prévision de la pollution dans l'équation de Burgers avec fonction d'erreur du modèle

Tran Thu Ha [a], Nguyen Hong Phong [a], François-Xavier Le Dimet [b], Hong Son Hoang [c,*]

[a] *Institute of Mechanics, 264 Doi Can, Graduate University of Science and Technology, Vietnam Academy of Science and Technology (VAST), 18 Hoang Quoc Viet, University of Engineering and Technology, VNU, 144 Xuan Thuy, Hanoï, Viet Nam*
[b] *Laboratoire Jean-Kuntzmann, 51, rue des Maths, 38400 Saint-Martin-d'Hères, France*
[c] *REC/HOM/SHOM, 42, avenue Gaspard-Coriolis, 31000 Toulouse, France*

ARTICLE INFO

Article history:
Received 12 September 2018
Accepted after revision 7 February 2019
Available online 8 April 2019

Keywords:
Burgers' equation
Water pollution
Data assimilation
Optimal method BFGS

Mots-clés :
Équation de Burgers
Pollution de l'eau
Assimilation de données
Méthode optimale BFGS

ABSTRACT

This article presents a correction method for a better resolution of the problem of estimating and predicting pollution, governed by Burgers' equations. The originality of the method consists in the introduction of an error function into the system's equations of state to model uncertainty in the model. The initial conditions and diffusion coefficients, present in the equations for pollution and concentration, and also those in the model error equations, are estimated by solving a data assimilation problem. The efficiency of the correction method is compared with that produced by the traditional method without introduction of an error function.
Three test cases are presented in this study in order to compare the performances of the proposed methods. In the first two tests, the reference is the analytical solution and the last test is formulated as part of the "twin experiment".
The numerical results obtained confirm the important role of the model error equation for improving the prediction capability of the system, in terms of both accuracy and speed of convergence.

RÉSUMÉ

Cet article présente une méthode de correction permettant de mieux résoudre le problème de l'estimation et de la prédiction de la pollution décrit par les équations de Burgers. L'originalité de la méthode consiste en l'introduction d'une fonction d'erreur dans le modèle d'état du système pour modéliser l'incertitude du modèle initial. Les conditions initiales et les coefficients de diffusion, présents dans les équations de pollution et de concentration, ainsi que ceux des équations d'erreur du modèle, sont estimés en résolvant un problème d'assimilation de données. L'efficacité de la méthode de correction est

* Corresponding author.
E-mail addresses: ttha@imech.vast.vn (T.T. Ha), hphongbk@gmail.com (N.H. Phong), fxld@yahoo.com (F.-X. Le Dimet), hhoang@shom.fr (H.S. Hoang).

https://doi.org/10.1016/j.crme.2019.02.002

comparée à celle offerte par la méthode traditionnelle sans introduction d'une fonction d'erreur.
Trois cas de tests sont présentés dans cette étude pour comparer les performances des méthodes utilisées. Dans les deux premiers tests, la référence est la solution analytique, et le dernier test est formulé dans le cadre de « l'expérience jumelle ». Les résultats numériques obtenus confirment le rôle important de l'équation d'erreur du modèle dans l'amélioration de la capacité de prédiction du système, en termes de précision et de rapidité de convergence de la méthode de correction.

1. Introduction

One of the greatest problems that the world is facing today is that of water pollution. A major scientific challenge is the ability to predict the evolution of an episode of pollution. To achieve this goal, we need to mix several sources of information like

- the mathematical model based on the equation of conservation;
- observations in situ or remote measurements;
- statistics on the field;
- images.

The numerical model, obtained from a set of mathematical equations, allows us to retrieve the principal structures of the flow. As there always exist differences between the model used and the physical process under consideration, observations constitute an essential source of information to correctly estimate the system's state and, as a consequence, to produce a better forecast. Combining the model with observations can be done, in an optimal way, by data assimilation algorithms. For the most recent progress in data assimilation in meteorology, oceanography and hydrology, see [14]. In particular, Variational Data Assimilation (VDA) is based on the idea of finding an optimal system trajectory, not in the functional space, but in the space of the initial state under the condition of a perfect model. Taking into account the model error in the VDA is one of the important steps in broadening the horizons of its application and in improving its performance. In this context, the questions of the propagation of error and of its impact on the final analysis are of importance and are studied in [4–6]. The following errors are typical in the study of DA problems:

- model errors (see [2]). Geophysical flows are governed by nonlinear laws and there exist interactions between the spatial and temporal scales. Namely,
  - numerical models require a truncation in both temporal and spatial scales and, consequently, a parameterization of the interactions with smallest scales (turbulence). These interactions are not explicit and need to be parameterized,
  - empirical laws are introduced into the model,
  - an other source of errors is due to the uncertainty in the specification of the model coefficients;
- observation errors (see [16]): they could be issued from errors in measurements, sampling errors... In many situations, the state variables are not observed directly and are estimated as a solution to some inverse problems.

Let us mention that, in many situations, the model and observation errors are dependent, which makes the estimation problem more complex.

It is important to emphasize that, in its traditional framework, the VDA is formulated as a strong constraint optimization problem, i.e. an optimization problem subject to (s.t.) the perfect dynamical system – the system without model error (ME). In this situation, only the initial system state is considered as a control vector (and, maybe, along with some system parameters). In this work, in addition to the initial state, the ME will be introduced as the unknown to be estimated. In fact, in practice, in numerical weather prediction in meteorology or oceanography, the numerical model used is never perfect, hence the introduction of the ME is beneficial for improving the forecasting capacity of the DA systems. And as it becomes clear from the numerical experiments to follow, a proper introduction of the ME equation will allow us to decrease considerably the estimation error. A brief outline on how the ME function (MEF) can be introduced in the VDA will be given in the Appendix.

In this paper, the hydraulic and pollution equations (originated from Burgers' equation) are used to compute the transport of pollution substances. It can be done if the initial values for the model are known and the model parameters are adequately specified. Since the parameters or initial values are not known (or very badly known), their approximations are used instead. One of simple procedures for approximating these values is to average the quantities produced by running the numerical model over a long time period. As these estimates are often approximate and if the model parameters are inadequately specified, the resulting solution is usually poorly estimated.

The objective of this paper is to show that there exists a possibility to improve considerably a solution to the pollution problem by introducing MEF into the model equation and solving the corresponding VDA s.t. the initial conditions and the diffusion coefficients as control variables (θ) [17]. Seeking an optimal solution for this problem is based on the optimal control theory [11], [12].

The following problems will be addressed in sections 2–4:

- solve the VDA problem over the interval $[t_1, t_2]$, i.e. minimizing the objective function E s.t. the control vector θ (it is supposed that we are given a set of measurements in the interval $[t_1, t_2]$);
- carry out a comparison study between the estimation error of the produced solution and those of the two other standard solutions, which will be presented in detail to show the effectiveness of the VDA-based solution.

2. Mathematical formulation of the problem

In this section, we formulate the two estimation problems.

2.1. Estimation problem with the error function (EF) E_u for Burgers' equation

Let $U = U(x,t)$ be the solution to Burgers' equation, with EF E_u,

$$\begin{cases} \dfrac{\partial U}{\partial t} + U\dfrac{\partial U}{\partial x} = \nu\dfrac{\partial^2 U}{\partial x^2} + G_u \cdot E_u, & x \in [L_0, L] \text{ and } t \in (t_1, t_2] \\ U = U_{\text{in}}(t) \text{ on } x = L_0 \\ \dfrac{\partial U}{\partial x} = 0 \text{ or } U = f_u \text{ on } x = L \\ U(t_1) = U_0 \end{cases} \tag{1}$$

The evolution of the pollutant concentration $C = C(x,t)$ is modeled by a one-dimensional advection diffusion equation with EF E_C:

$$\begin{cases} \dfrac{\partial C}{\partial t} + U\dfrac{\partial C}{\partial x} = \eta\dfrac{\partial^2 C}{\partial x^2} + G_C \cdot E_C, & x \in [L_0, L] \text{ and } t \in (t_1, t_2] \\ C = C_{\text{in}} \text{ on } x = L_0 \\ \dfrac{\partial C}{\partial x} = 0 \text{ or } C = f_c \text{ on } x = L \\ C(t_1) = C_0, \quad x \in [L_0, L] \end{cases} \tag{2}$$

Here the diffusion coefficients $\eta \in Y_p$ and $\nu \in Y_p$, where Y_p is the space of parameters, are supposed to be constants; $E_u \in \wp_u$, $E_C \in \wp_C$, $u \in X_u$, $C \in X_C$ with $\wp_u$, $\wp_C$, X_u and X_C are the Hilbert spaces; $f_u(t) \in X_u$ and $f_c(t) \in X_C$ are functions of time t $U_0 \in X_u$ and $C_0 \in X_C$ are the initial conditions.

Let us introduce the Hilbert spaces $Y_C = L_2(X_C, t_1, t_2)$, $Y_U = L_2(X_u, t_1, t_2)$ with $\|\,.\,\|_{Y_u} = (.,.)^{1/2}_{Y_u}$ and $\|\,.\,\|_{Y_C} = (.,.)^{1/2}_{Y_C}$. The operators $G_u : Y_U \to Y_{U_{\text{obs}}}$, $G_C : Y_C \to Y_{C_{\text{obs}}}$ are linearly bounded. Here U_{obs} and C_{obs} are the measurement values of U and C satisfying $U_{\text{obs}} = H_u U$, $C_{\text{obs}} = H_C C$. In the experiments in the next sections, it is assumed that we observe U, C at several spatial points. The operators G_u, G_C are defined simply as $G_u = H_u^* H_u$, $G_C = H_c^* H_c$, where H_u^*, H_C* are the adjoint operators for H_u and H_C.

We assume that EF, E_u, and E_C are satisfying the following equations:

$$\begin{cases} \dfrac{\partial E_u}{\partial t} = \dfrac{\partial}{\partial x}\left(K_u(x)\dfrac{\partial E_u}{\partial x}\right), \ x \in [L_0, L] \text{ and } t \in (t_1, t_2] \\ E_u = 0 \text{ on } x = L_0 \\ E_u = 0 \text{ on } x = L \\ E_u(t_1) = V_u \end{cases} \tag{3}$$

$$\begin{cases} \dfrac{\partial E_C}{\partial t} = \dfrac{\partial}{\partial x}\left(K_C(x)\dfrac{\partial E_C}{\partial x}\right), \ x \in [L_0, L] \text{ and } t \in (t_1, t_2] \\ E_C = 0 \text{ on } x = L_0 \\ E_C = 0 \text{ on } x = L \\ E_C(t_1) = V_C \end{cases} \tag{4}$$

Here $K_u \succ 0 \in Y_p$, $K_C \succ 0 \in Y_p$ are the diffusion coefficients, $V_u \in \wp_u$, $V_C \in \wp_C$ are the initial condition values of Eqs. (3)–(4), respectively. Their values will be defined by solving the following optimization problem.

Let θ denote a vector consisting of all variables U_0, C_0, V_u, V_C, ν, η, K_u, K_C. Introduce the objective function

$$J(\theta)=\frac{1}{2}\parallel G_u U-U_{\rm obs}\parallel^2_{Y_{U_{\rm obs}}}+\frac{1}{2}\parallel G_C C-C_{\rm obs}\parallel^2_{Y_{C_{\rm obs}}}+\frac{1}{2}\parallel U_0-\bar{U}_0\parallel^2_{L_2(X_U)}+\frac{1}{2}\parallel C_0-\bar{C}_0\parallel^2_{L_2(X_C)}$$
$$+\frac{1}{2}\parallel \nu-\nu_0\parallel^2+\frac{1}{2}\parallel \eta-\eta_0\parallel^2+\frac{1}{2}\int_{t_1}^{t_2}\parallel E_u\parallel^2_{L_2(\wp_u)}\,\mathrm{d}t+\frac{1}{2}\int_{t_1}^{t_2}\parallel E_C\parallel^2_{L_2(\wp_C)}\,\mathrm{d}t+\frac{1}{2}\parallel V_u-V_{u,0}\parallel^2_{L_2(\wp_u)}$$
$$+\frac{1}{2}\parallel V_C-V_{C,0}\parallel^2_{L_2(\wp_C)}+\frac{1}{2}\parallel K_u-K_{u,0}\parallel^2_{Y_p}+\frac{1}{2}\parallel K_C-K_{C,0}\parallel^2_{Y_p}. \tag{5}$$

Here $\bar{U}_0$, $\bar{C}_0$, ν_0, η_0, $V_{u,0}$, $V_{C,0}$, $K_{u,0}$, $K_{C,0}$ are a priori given.

The VDA, considered here, consists in minimizing $J(\theta)$ (5) s.t. (1)–(4), where θ is a control vector, i.e.

$$\left\{\begin{array}{rcl}
\dfrac{\partial U}{\partial t}+U\dfrac{\partial U}{\partial x} &=& \nu\dfrac{\partial^2 U}{\partial x^2}+G_u\cdot E_u \ x\in[L_0,L] \text{ and } t\in(t_1,t_2]\\
\dfrac{\partial C}{\partial t}+U\dfrac{\partial C}{\partial x} &=& \eta\dfrac{\partial^2 C}{\partial x^2}+G_C\cdot E_C \ x\in[L_0,L] \text{ and } t\in(t_1,t_2]\\
\dfrac{\partial E_u}{\partial t} &=& \dfrac{\partial}{\partial x}\left(K_u(x)\dfrac{\partial E_u}{\partial x}\right) \ x\in[L_0,L] \text{ and } t\in(t_1,t_2]\\
\dfrac{\partial E_C}{\partial t} &=& \dfrac{\partial}{\partial x}\left(K_C(x)\dfrac{\partial E_C}{\partial x}\right) \ x\in[L_0,L] \text{ and } t\in(t_1,t_2]\\
U &=& U_{\rm in} \text{ on } x=L_0\\
C &=& C_{\rm in} \text{ on } x=L_0\\
\dfrac{\partial C}{\partial x} &=& 0 \text{ or } C=f_c \text{ on } x=L\\
\dfrac{\partial U}{\partial x} &=& 0 \text{ or } U=f_u \text{ on } x=L\\
E_u &=& 0 \text{ on } x=L_0\\
E_u &=& 0 \text{ on } x=L\\
E_C &=& 0 \text{ on } x=L_0\\
E_C &=& 0 \text{ on } x=L\\
U(t_1) &=& U_0\\
C(t_1) &=& C_0\\
E_u(t_1) &=& V_u\\
E_C(t_1) &=& V_C\\
J(\theta^*) &=& \operatorname{Arg}\min\limits_{\theta} J(\theta)
\end{array}\right. \tag{6}$$

To solve the optimality system, we need to compute the gradient of the cost function J with respect to the control variables U_0, C_0, ν, η, V_u, V_C, K_u, K_C. For this purpose, we consider a direction $(u, c, \tilde{\nu}, \tilde{\eta}, \nu_u, \nu_c, k_u, k_c)$, in which we will compute the Gateaux derivatives.

Let us introduce the adjoint variables P_u, P_C, Q_u, Q_C, which are the solutions to the systems describing the adjoint model (cf., [13]),

$$\left\{\begin{array}{rcl}
\dfrac{\partial P_u}{\partial t} &=& -U\dfrac{\partial P_u}{\partial x}-\nu\dfrac{\partial^2 P_u}{\partial x^2}+P_C\dfrac{\partial C}{\partial x}+G_u^{\mathsf{T}}\cdot(G_u U-U_{\rm obs}),\, x\in[L_0,L],\, t\in[t_1,t_2)\\
P_u &=& 0 \qquad \text{on } x=L_0\\
\nu\dfrac{\partial P_u}{\partial x}+UP_u &=& 0 \text{ if } \dfrac{\partial U}{\partial x}=0 \qquad \text{on } x=L\\
P_u &=& 0 \text{ if } U=f_u \qquad \text{on } x=L\\
P_u(t_2) &=& 0
\end{array}\right. \tag{7}$$

$$\begin{cases} \dfrac{\partial P_C}{\partial t} = -\dfrac{\partial U P_C}{\partial x} - \eta \dfrac{\partial^2 P_C}{\partial x^2} + G_C^{\mathsf{T}} \cdot (G_C C - C_{\text{obs}}) \ x \in [L_0, L] \text{ and } t \in [t_1, t_2) \\ P_C = 0 \quad \text{on } x = L_0 \\ \eta \dfrac{\partial P_C}{\partial x} + U P_C = 0 \text{ if } \dfrac{\partial C}{\partial x} = 0 \quad \text{on } x = L \\ P_C = 0 \text{ if } C = f_C \quad \text{on } x = L \\ P_C(t_2) = 0 \end{cases} \tag{8}$$

$$\begin{cases} \dfrac{\partial Q_u}{\partial t} = \dfrac{\partial}{\partial x}\left(K_u(x) \dfrac{\partial Q_u}{\partial x}\right) - G_u^{\mathsf{T}} \cdot P_u + E_u \quad x \in [L_0, L] \text{ and } t \in [t_1, t_2) \\ Q_u = 0 \quad \text{on } x = L_0 \\ Q_u = 0 \quad \text{on } x = L \\ Q_u(t_2) = 0 \end{cases} \tag{9}$$

$$\begin{cases} \dfrac{\partial Q_C}{\partial t} = \dfrac{\partial}{\partial x}\left(K_C(x) \dfrac{\partial Q_C}{\partial x}\right) - G_C^{\mathsf{T}} \cdot P_C + E_C \quad x \in [L_0, L] \text{ and } t \in [t_1, t_2) \\ Q_C = 0 \quad \text{on } x = L_0 \\ Q_C = 0 \quad \text{on } x = L \\ Q_C(t_2) = 0 \end{cases} \tag{10}$$

From this we deduce the gradient of the cost function J (5), which is:

$$\nabla J(U_0, C_0, \nu, \eta, V_u, V_C, K_u, K_C) = \left(J'_{U_0}, J'_{C_0}, J'_\nu, J'_\eta, J'_{V_u}, J'_{V_C}, J'_{K_u}, J'_{K_C}\right) \tag{11}$$

where:

$$\begin{cases} J'_{U_0} = U_0 - \bar{U}_0 - P_u(t_1) \\ J'_{C_0} = C_0 - \bar{C}_0 - P_C(t_1) \\ J'_\nu = \nu - \nu_0 + \dfrac{1}{L - L_0} \displaystyle\int_{t_1}^{t_2} \left(\dfrac{\partial U}{\partial x}, \dfrac{\partial P_u}{\partial x}\right) \mathrm{d}t \\ J'_\eta = \eta - \eta_0 + \dfrac{1}{L - L_0} \displaystyle\int_{t_1}^{t_2} \left(\dfrac{\partial C}{\partial x}, \dfrac{\partial P_C}{\partial x}\right) \mathrm{d}t \\ J'_{V_u} = V_u - V_{u,0} - Q_u(t_1) \\ J'_{V_C} = V_C - V_{C,0} - Q_C(t_1) \\ J'_{K_u} = K_u - K_{u,0} + \displaystyle\int_{t_1}^{t_2} \dfrac{\partial E_u}{\partial x} \dfrac{\partial Q_u}{\partial x} \mathrm{d}t \\ J'_{K_C} = K_C - K_{C,0} + \displaystyle\int_{t_1}^{t_2} \dfrac{\partial E_C}{\partial x} \dfrac{\partial Q_C}{\partial x} \mathrm{d}t \end{cases} \tag{12}$$

Using $\nabla J(U_0, C_0, \nu, \eta, V_u, V_C, K_u, K_C)$, defined by the formula (11), the optimal value for θ^* can be computed by solving the optimization problem (6) on the basis of the BFGS method (see [2], [10]). Eqs. (1)–(4) are solved by s.t. $U_0 = U_0^*$, $C_0 = C_0^*$, $\nu = \nu^*$, $\eta = \eta^*$, $V_u = V_u^*$, $V_C = V_C^*$, $K_u = K_u^*$, $K_C = K_C^*$. These values will be used in the model to produce the forecast in section 3.

In the next subsection, the VDA problem is formulated for Burgers' equation without error function.

2.2. The classical correction problem of Burgers' equation

Assume that the one-dimension velocity $U = U(x,t)$ verifies Burgers' equation:

$$\begin{cases} \dfrac{\partial U}{\partial t} + U \dfrac{\partial U}{\partial x} = \nu \dfrac{\partial^2 U}{\partial x^2} \quad x \in [L_0, L] \text{ and } t \in (t_1, t_2] \\ U = U_{\text{in}} \text{ on } x = L_0 \\ \dfrac{\partial U}{\partial x} = 0 \text{ or } U = f_u \text{ on } x = L \\ U(t_1) = U_0 \end{cases} \tag{13}$$

The evolution of the pollutant concentration $C = C(x,t)$ is modeled by a one-dimensional advection diffusion equation:

$$\begin{cases} \dfrac{\partial C}{\partial t} + U\dfrac{\partial C}{\partial x} &= \eta \dfrac{\partial^2 C}{\partial x^2} \qquad x \in [L_0, L] \text{ and } t \in (t_1, t_2] \\ C &= C_{\text{in}} \text{ on } x = L_0 \\ \dfrac{\partial C}{\partial x} &= 0 \text{ or } C = f_c \text{ on } x = L \\ C(t_1) &= C_0 \end{cases} \tag{14}$$

Let θ denote a vector consisting of the initial condition values U_0, C_0 and diffusion coefficients ν, η. The cost function is defined by:

$$\tilde{J}(\theta) = \frac{1}{2} \parallel G_u U - U_{\text{obs}} \parallel^2_{Y_{U_{\text{obs}}}} + \frac{1}{2} \parallel G_C C - C_{\text{obs}} \parallel^2_{Y_{C_{\text{obs}}}} + \frac{1}{2} \parallel U_0 - \bar{U}_0 \parallel^2_{L_2(X_U)} + \frac{1}{2} \parallel C_0 - \bar{C}_0 \parallel^2_{L_2(X_C)} \\ + \frac{1}{2} \parallel \nu - \nu_0 \parallel^2 + \frac{1}{2} \parallel \eta - \eta_0 \parallel^2 \tag{15}$$

where $\bar{U}_0$, $\bar{C}_0$, ν_0, η_0 are given.

As before, the VDA problem is formulated as the minimization of $\tilde{J}(\theta)$ s.t. (13)–(14), i.e.

$$\begin{cases} \dfrac{\partial U}{\partial t} + U\dfrac{\partial U}{\partial x} &= \nu \dfrac{\partial^2 U}{\partial x^2} \; x \in [L_0, L] \text{ and } t \in (t_1, t_2] \\ \dfrac{\partial C}{\partial t} + U\dfrac{\partial C}{\partial x} &= \eta \dfrac{\partial^2 C}{\partial x^2} \; x \in [L_0, L] \text{ and } t \in (t_1, t_2] \\ U &= U_{\text{in}}, \text{ on } x = L_0 \\ C &= C_{\text{in}}, \text{ on } x = L_0 \\ \dfrac{\partial C}{\partial x} &= 0 \text{ or } C = f_c \text{ on } x = L \\ \dfrac{\partial U}{\partial x} &= 0 \text{ or } U = f_u \text{ on } x = L \\ U(t_1) &= U_0 \\ C(t_1) &= C_0 \\ \tilde{J}(\theta^*) &= \operatorname{Arg}\min_{\theta} \tilde{J}(\theta) \end{cases} \tag{16}$$

The gradient of cost function $\tilde{J}$ is now

$$\nabla \tilde{J}(U_0, C_0, \nu, \eta) = \left(\tilde{J}'_{U_0}, \tilde{J}'_{C_0}, \tilde{J}'_{\nu}, \tilde{J}'_{\eta} \right) \tag{17}$$

where

$$\begin{cases} \tilde{J}'_{U_0} &= U_0 - \bar{U}_0 - P_u(t_1) \\ \tilde{J}'_{C_0} &= C_0 - \bar{C}_0 - P_C(t_1) \\ \tilde{J}'_{\nu} &= \nu - \nu_0 + \dfrac{1}{L - L_0} \displaystyle\int_{t_1}^{t_2} \left(\dfrac{\partial U}{\partial x}, \dfrac{\partial P_u}{\partial x} \right) \mathrm{d}t \\ \tilde{J}'_{\eta} &= \eta - \eta_0 + \dfrac{1}{L - L_0} \displaystyle\int_{t_1}^{t_2} \left(\dfrac{\partial C}{\partial x}, \dfrac{\partial P_C}{\partial x} \right) \mathrm{d}t \end{cases} \tag{18}$$

Here, P_u and P_C are the solutions to Eqs. (7) and (8).

As before, the solution to the problem (16) is computed using the BFGS method (see [2], [10]). Eqs. (13)–(14) are solved by s.t. $U_0 = U_0^*$, $C_0 = C_0^*$, $\nu = \nu^*$, $\eta = \eta^*$. The optimal values of ν, η, $U(t_2)$, and $C(t_2)$ will be used in the model to produce the forecasts U, C for the forecasting time period $[t_2, t_3]$.

3. Forecast problem

The forecast problem for the future time period $[t_2,\ t_3]$ consists in solving the following system of equations s.t. the optimal values of ν, η and $\hat{U}_0 = U(t_2)$, $\hat{C}_0 = C(t_2)$ (obtained in the previous section):

$$\begin{cases} \dfrac{\partial U}{\partial t} + U\dfrac{\partial U}{\partial x} &= \nu\dfrac{\partial^2 U}{\partial x^2} \; x \in [L_0, L] \text{ and } t \in (t_2, t_3] \\ \dfrac{\partial C}{\partial t} + U\dfrac{\partial C}{\partial x} &= \eta\dfrac{\partial^2 C}{\partial x^2} \; x \in [L_0, L] \text{ and } t \in (t_2, t_3] \\ U &= U_{\text{in}}, \text{ on } x = L_0 \\ C &= C_{\text{in}}, \text{ on } x = L_0 \\ \dfrac{\partial C}{\partial x} &= 0 \text{ or } C = f_c \text{ on } x = L \\ \dfrac{\partial U}{\partial x} &= 0 \text{ or } U = f_u \text{ on } x = L \\ U(t_2) &= \hat{U}_0 \\ C(t_2) &= \hat{C}_0 \end{cases} \tag{19}$$

4. Numerical examples: test cases

In order to see the effect of the introduced EF E_u, E_C, and the parameter estimation, three test cases will be considered:

- in the first test case, we consider Burgers' equation for velocity with boundary condition and known analytical solution;
- in the second test case, we study the advection equation for concentration with boundary condition that has a known analytical solution;
- in the third test case, the problem presented in section 2 is tested in the framework of the twin experiment.

In all three test cases, the guess values of the initial conditions and of the diffusion coefficients are quite different from those used in the reference models.

4.1. Test case 1: Correction experiment for Burgers' equation

For the time period $[t_1, t_2]$, we introduce the classical Burgers' equation:

$$\begin{cases} \dfrac{\partial U}{\partial t} + U\dfrac{\partial U}{\partial x} &= \nu\dfrac{\partial^2 U}{\partial x^2} \qquad x \in [0, 1] \text{ and } t \in (t_1, t_2] \\ U &= 0 \qquad \text{on } x = 0 \\ U &= \dfrac{1}{t} - \dfrac{\pi}{t}\tanh\left(\dfrac{\pi}{2\,\nu\,t}\right) \qquad \text{on } x = 1 \\ U(t_1) &= U_0 \end{cases} \tag{20}$$

For the next time period $[t_2, t_3]$, we consider the solution to the equation:

$$\begin{cases} \dfrac{\partial U}{\partial t} + U\dfrac{\partial U}{\partial x} &= \nu\dfrac{\partial^2 U}{\partial x^2} \qquad x \in [0, 1] \text{ and } t \in (t_2, t_3] \\ U &= 0 \qquad \text{on } x = 0 \\ U &= \dfrac{1}{t} - \dfrac{1}{t} - \dfrac{\pi}{t}\tanh\left(\dfrac{\pi}{2\,\nu\,t}\right) \qquad \text{on } x = 1 \\ U(t_2) &= \hat{U}_0 \end{cases} \tag{21}$$

The following data set is used: $t_0 = 0.12$ s, $t_1 = 0.241$ s, $t_2 = 1.241$ s, $t_3 = 2.041$ s, $\Delta t = 0.0001$ s. The measurements are taken at points : $x = 0.2$ m, $x = 0.4$ m, $x = 0.9$ m. The performances of the different solutions are tested at point $x = 0.5$ m.

Consider the four models below.

- 1. *Reference model* (RM). The function

$$U(x,t) = \frac{x}{t} - \frac{1}{t} - \frac{\pi}{t}\tanh\left(\frac{\pi x}{2\,\bar{\nu}\,t}\right) \tag{22}$$

is the exact solution to the equation (see [1]):

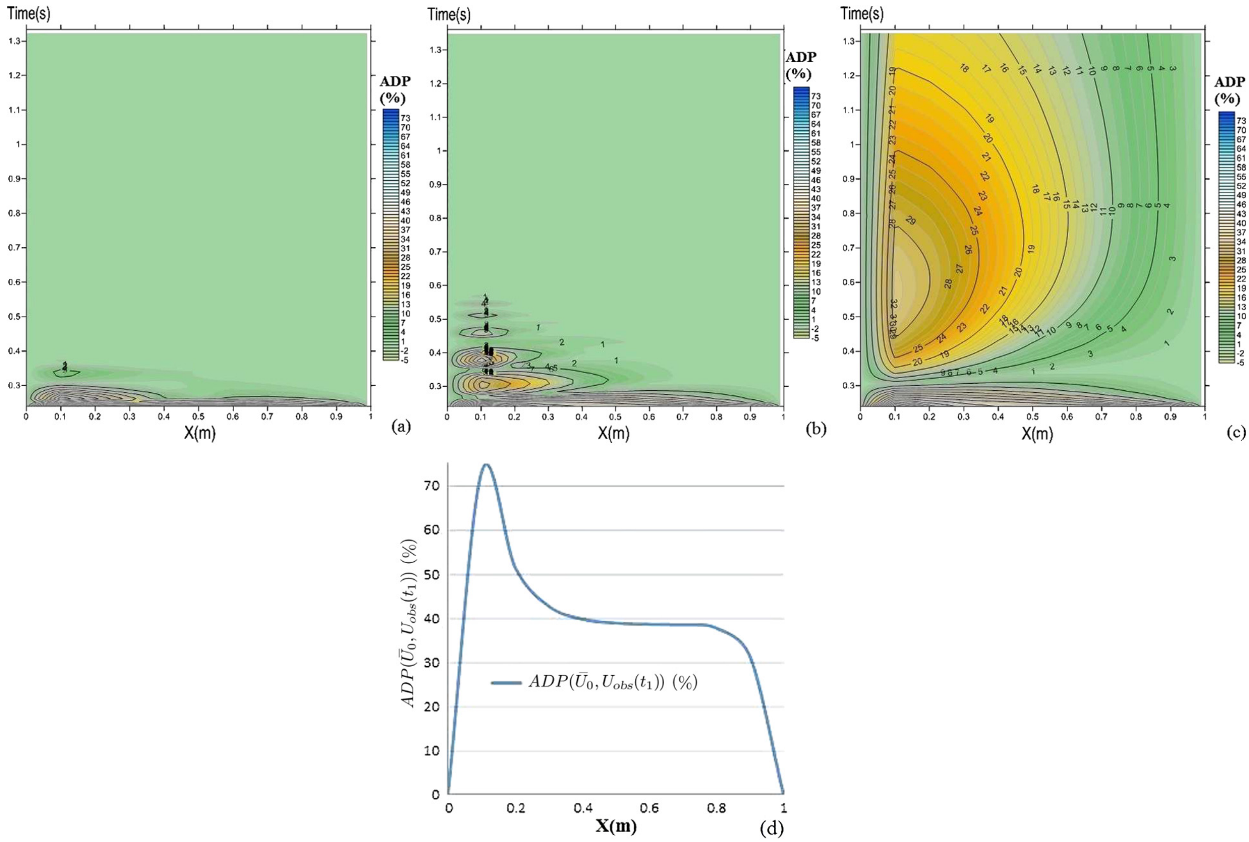

Fig. 1. Test case 1. Panels (a)–(c): the spatio-temporal $ADP(velocity)$ between the three different runs MEF (a), MNEF (b), EM (c), and RM. It is seen that compared to EM, the VDA allows MNEF to reduce significantly the estimation error. The effect of the introduced EF is clearly visible, comparing (a) with (b) and (c). The spatial $ADP(velocity)$ between $\bar{U}_0$ and $U_{\text{obs}}(t_1)$, representing the error in the initial condition, is displayed in panel (d).

$$\begin{cases} \dfrac{\partial U}{\partial t} + U\dfrac{\partial U}{\partial x} = \bar{\nu}\dfrac{\partial^2 U}{\partial x^2}, & x \in [0,1] \text{ and } t \in (t_1, t_3] \\ U = 0 & \text{on } x = 0 \\ U = \dfrac{1}{t} - \dfrac{\pi}{t}\tanh\left(\dfrac{\pi}{2\,\bar{\nu}\,t}\right) & \text{on } x = 1 \\ U(t_1, x) = \dfrac{x}{t_1} - \dfrac{\pi}{t_1}\tanh\left(\dfrac{\pi x}{2\,\bar{\nu}\,t_1}\right) \end{cases} \tag{23}$$

The solution U_{obs}, obtained by solving (22) for the time period $[t_1, t_3]$ s.t. $\bar{\nu} = 1$ m^2/s, is referred to as a *RM solution* (or *reference solution*).

– 2. Introduce an *erroneous model* (EM) (its EM solution is denoted by U_{EM}), which is given by (20) s.t.
  – $\nu = 1.5$ m^2/ s,
  – $U_0 = \bar{U}_0$ where $\bar{U}_0$ is defined by the following function:

$$\bar{U}_0 = \frac{1}{t_1 - t_0}\int_{t_0}^{t_1}\left[\frac{x}{t} - \frac{1}{t} - \frac{\pi}{t}\tanh\left(\frac{\pi x}{2\,\nu\,t}\right)\right]\mathrm{d}t \tag{24}$$

Introduce the Absolute Difference Percent (ADP) as a measure of the difference between two variables a and b

$$ADP(a, b) = |a - b| * 100/|b|$$

To see how the initial conditions are different in EM and RM, in the Fig. 1 we show the spatial $ADP(\bar{U}_0, U_{\text{obs}}(t_1))$ (i.e. on the interval $x \in [0:1]$). One sees that the maximum ADP level is higher than 70%. As to the diffusion coefficients ν and $\bar{\nu}$, they are also quite different ($\nu = 1.5$ m^2/s, $\bar{\nu} = 1$ m^2/s).

The difference $ADP(U_{\text{EM}}, U_{\text{obs}})$ between the two solutions, produced by EM and RM, is displayed in Fig. 1c over the time period $[t_1, t_2]$.

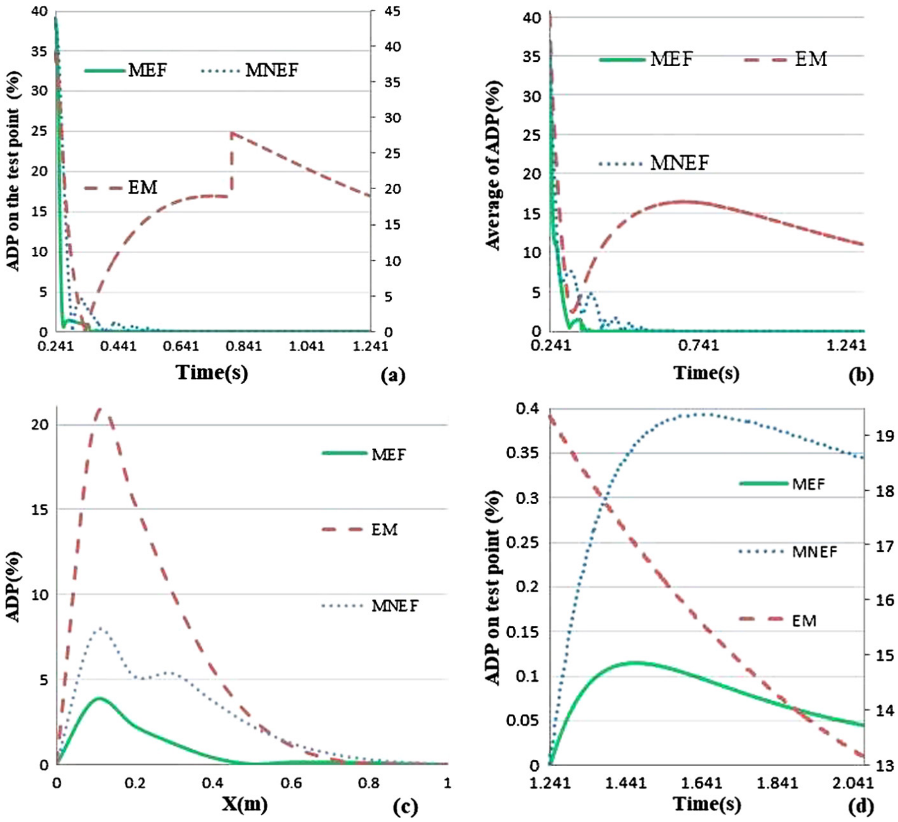

Fig. 2. Test case 1. (a) The curves MEF, MNEF and EM show the $ADP(velocity)$ between three runs MEF, MNEF, EM and RM at the test point. The values of EM are projected onto the right vertical axis. (b) Time averages of the curves in (a). (c) Spatial $ADP(velocity)$ between three runs MEF, MNEF, EM, and RM for the time moment $t = 0.35$ s. (d) The curves MEF, MNEF and EM express the $ADP(velocity)$ between MEF, MNEF, EM and RM at the test point for the forecasting time period $[t_2, t_3]$. The EM values are projected onto the right vertical axis.

To see how the error affects the forecast, we integrate (21) over the next time period $[t_2, t_3]$ s.t. $\hat{U}_0 = U_{\text{EM}}(t_2)$. The $ADP(U^{\text{f}}_{\text{EM}}, U_{\text{obs}})$ between the obtained forecast solution (denoted as U^{f}_{EM}) and the RM solution (reference) at the test point is represented by the dashed red curve in Fig. 2d.

– 3. Introduce the MEF model (model, including EF E_u): let us consider the system of equations

$$\begin{cases} \dfrac{\partial U}{\partial t} + U\dfrac{\partial U}{\partial x} = \nu\dfrac{\partial^2 U}{\partial x^2} + G_u \cdot E_u, & x \in [0,1] \text{ and } t \in (t_1, t_2] \\ \dfrac{\partial E_u}{\partial t} = \dfrac{\partial}{\partial x}\left(K_u(x)\dfrac{\partial E_u}{\partial x}\right), & x \in [0,1] \text{ and } t \in (t_1, t_2] \\ U = 0 & \text{on } x = 0 \\ U = \dfrac{1}{t} - \dfrac{\pi}{t}\tanh\left(\dfrac{\pi}{2\nu t}\right) & \text{on } x = 1 \\ U(t_1) = U_0 & \\ E_u = 0 & \text{on } x = 0 \\ E_u = 0 & \text{on } x = 1 \\ E_u(t_1) = V_u & \end{cases} \tag{25}$$

We are interested in adjusting U_0, V_u, ν, and K_u in such a way to make the solution U as close as possible to the RM solution U_{obs}. For this purpose, we introduce the cost function:

$$\hat{J}(U_0, \nu, V_u, K_u) = \frac{1}{2} \parallel G_u U - U_{\text{obs}} \parallel^2_{Y_{U_{\text{obs}}}} + \frac{1}{2} \parallel U_0 - \bar{U}_0 \parallel^2_{L_2(X_U)} + \frac{1}{2} \parallel \nu - \nu_0 \parallel^2 + \frac{1}{2}\int_{t_1}^{t_2} \parallel E_u \parallel^2_{L_2(\wp_u)} \, \mathrm{d}t$$
$$+ \frac{1}{2} \parallel V_u - V_{u,0} \parallel^2_{L_2(\wp_u)} + \frac{1}{2} \parallel K_u - K_{u,0} \parallel^2_{Y_p} \tag{26}$$

where $\bar{U}_0$, ν_0, $V_{u,0}$ and $K_{u,0}$ are given.

Let us consider the problem of minimizing J_1 s.t. the model as a constraint:

$$\begin{cases} \dfrac{\partial U}{\partial t} + U\dfrac{\partial U}{\partial x} = \nu\dfrac{\partial^2 U}{\partial x^2} + G_u \cdot E_u & x \in [0,1] \text{ and } t \in (t_1, t_2] \\ \dfrac{\partial E_u}{\partial t} = \dfrac{\partial}{\partial x}\left(K_u(x)\dfrac{\partial E_u}{\partial x}\right) & x \in [0,1] \text{ and } t \in (t_1, t_2] \\ U = 0 & \text{on } x = 0 \\ U = \dfrac{1}{t} - \dfrac{\pi}{t}\tanh\left(\dfrac{\pi}{2\nu t}\right) & \text{on } x = 1 \\ U(t_1) = U_0 \\ E_u = 0 & \text{on } x = 0 \\ E_u = 0 & \text{on } x = 1 \\ E_u(t_1) = V_u \\ \hat{J}(U_0^*, \nu^*, V_u^*, K_u^*) = \text{Arg}\min_{U_0, \nu, V_u, K_u} \hat{J}(U_0, \nu, V_u, K_u) \end{cases} \tag{27}$$

The gradient of the cost function is

$$\nabla\hat{J}(U_0, \nu, V_u, K_u) = \left(\hat{J}'_{U_0}, \hat{J}'_{\nu}, \hat{J}'_{V_u}, \hat{J}'_{K_u}\right) \tag{28}$$

where $\hat{J}'_{U_0}$, $\hat{J}'_{\nu}$, $\hat{J}'_{V_u}$, and $\hat{J}'_{K_u}$ are defined by

$$\begin{cases} \hat{J}'_{U_0} = U_0 - \bar{U}_0 - \bar{P}_u(t_1) \\ \hat{J}'_{\nu} = \nu - \nu_0 + \displaystyle\int_{t_1}^{t_2} \left(\dfrac{\partial U}{\partial x}, \dfrac{\partial \bar{P}_u}{\partial x}\right) \mathrm{d}t \\ \hat{J}'_{V_u} = V_u - V_{u,0} - \bar{Q}_u(t_1) \\ \hat{J}'_{K_u} = K_u - K_{u,0} + \displaystyle\int_{t_1}^{t_2} \dfrac{\partial E_u}{\partial x}\dfrac{\partial \bar{Q}_u}{\partial x}\,\mathrm{d}t \end{cases} \tag{29}$$

where $\bar{P}_u$ and $\bar{Q}_u$ are the solutions to the system:

$$\begin{cases} \dfrac{\partial \bar{P}_u}{\partial t} = -U\dfrac{\partial \bar{P}_u}{\partial x} - \nu\dfrac{\partial^2 \bar{P}_u}{\partial x^2} + G_u^{\intercal}\cdot(G_u U - U_{\text{obs}}), & x \in [0,1], t \in [t_1, t_2) \\ \bar{P}_u = 0 & \text{on } x = 0 \\ \bar{P}_u = 0 & \text{on } x = 1 \\ \bar{P}_u(t_2) = 0 \end{cases} \tag{30}$$

$$\begin{cases} \dfrac{\partial \bar{Q}_u}{\partial t} = \dfrac{\partial}{\partial x}\left(K_u(x)\dfrac{\partial \bar{Q}_u}{\partial x}\right) - G_u^{\intercal}\cdot\bar{P}_u + E_u & x \in [0,1] \text{ and } t \in [t_1, t_2) \\ \bar{Q}_u = 0 & \text{on } x = 0 \\ \bar{Q}_u = 0 & \text{on } x = 1 \\ \bar{Q}_u(t_2) = 0 \end{cases} \tag{31}$$

The problem (27) is solved by s.t. $\nu_0 = 1.5\,\bar{\nu} = 1.5$ m^2/s, $K_{u,0} = 1$ m^2/s, with $\bar{U}_0$ defined by (24) and $V_{u,0}$ chosen as

$$V_{u,0} = \begin{cases} U_{\text{obs}}(t_1) - \bar{U}_0 & \text{on measurement points} \\ 0 & \text{on no-measurement points} \end{cases} \tag{32}$$

We have applied the BFGS algorithm (see [2], [10]) to estimate the optimal parameters U_0^*, ν^*, V_u^*, K_u^*.
The optimal value for ν^* is denoted by ν^*_{MEF} and is equal to $\nu^*_{\text{MEF}} = 1.001$ m^2/s.
Solving the system of Eqs. (25) s.t. $U_0 = U_0^*$, $V_u = V_u^*$, $\nu = \nu^*_{\text{MEF}}$ and $K_u = K_u^*$ yields the solution (denoted as U_{MEF}). The $ADP(U_{\text{MEF}}, U_{\text{obs}})$, for the time period $[t_1, t_2]$, is displayed in Fig. 1a.
We have produced the forecast solution $U^{\text{f}}_{\text{MEF}}$ for the next future time period $[t_2, t_3]$ by solving the problem (21) s.t. $\nu = \nu^*_{\text{MEF}} = 1.001$ m^2/s, $\hat{U}_0 = U_{\text{MEF}}(t_2)$. In Fig. 2d, the green curve represents the $ADP(U^{\text{f}}_{\text{MEF}}, U_{\text{obs}})$ between the forecast solution of MEF and the RM solution at the test point.

– 4. Let us examine the situation without inclusion of EF E_u in the model (denoted as MNEF).
As before, we try to adjust the initial condition U_0 and the diffusion coefficient ν in the system of Eqs. (20) to produce a solution U as close as possible to the reference solution U_{obs} by solving the corresponding optimization problem. It is done by introducing the cost function:

$$\bar{J}(U_0,\nu)=\frac{1}{2}\parallel G_u U-U_{\text{obs}}\parallel^2_{Y_{U_{\text{obs}}}}+\frac{1}{2}\parallel U_0-\bar{U}_0\parallel^2_{L_2(X_U)}+\frac{1}{2}\parallel \nu-\nu_0\parallel^2 \tag{33}$$

where $\bar{U}_0$, ν_0 are given.
Then the corresponding optimization problem is to minimize (33) s.t.

$$\begin{cases} \dfrac{\partial U}{\partial t}+U\dfrac{\partial U}{\partial x} = \nu\dfrac{\partial^2 U}{\partial x^2} & x\in[0,1] \text{ and } t\in(t_1,t_2] \\ U = 0 & \text{on } x=0 \\ U = \dfrac{1}{t}-\dfrac{\pi}{t}\tanh\left(\dfrac{\pi}{2\,\nu\,t}\right) & \text{on } x=1 \\ U(t_1) = U_0 \\ \bar{J}(U_0^*,\nu^*) = \operatorname{Arg}\min\limits_{U_0,\nu}\bar{J}(U_0,\nu) \end{cases} \tag{34}$$

The gradient of the cost function is

$$\nabla\bar{J}(U_0,\nu)=\left(\bar{J}'_{U_0},\bar{J}'_{\nu}\right) \tag{35}$$

Here, $\bar{J}'_{U_0}$ and $\bar{J}'_{\nu}$ are defined by

$$\begin{cases} \bar{J}'_{U_0} = U_0-\bar{U}_0-\bar{P}_u(t_1) \\ \bar{J}'_{\nu} = \nu-\nu_0+\displaystyle\int_{t_1}^{t_2}\left(\frac{\partial U}{\partial x},\frac{\partial \bar{P}_u}{\partial x}\right)\mathrm{d}t \end{cases} \tag{36}$$

where $\bar{P}_u$ is the solution to the system of Eqs. (30).
The problem (34) is solved by s.t. $\nu_0=1.5\,\bar{\nu}=1.5$ m^2/ s and $\bar{U}_0$ defined by (24). The optimal values U_0^*, ν^* are obtained by applying the BFGS algorithm (see [2], [10]). For the further convenience, ν^* is denoted as ν^*_{MNEF}.
Let U_{MNEF} be the solution obtained by solving the system of Eqs. (20) (model without including EF) s.t. $U_0=U_0^*$ and $\nu=\nu^*_{\text{MNEF}}$. The Fig. 1b shows the $ADP(U_{\text{MNEF}},U_{\text{obs}})$ over the time period $[t_1,t_2]$.
For the next time period $[t_2,t_3]$, the problem (21) s.t. $\nu=\nu^*_{\text{MNEF}}=1.012$ m^2/s and $\hat{U}_0=U_{\text{MNEF}}(t_2)$ is solved. Its solution (forecast) is denoted as $U^{\text{f}}_{\text{MNEF}}$. The $ADP(U^{\text{f}}_{\text{MNEF}},U_{\text{obs}})$, at the test point, is presented by the dot blue curve in Fig. 2d.

Compared to the solutions produced by MNEF and MEF, the error in EM is much higher (see Figs. 1a–1c). The role of EF is clearly visible since the error in MEF (see Fig. 1a) is significantly lower than that in MNEF (see Fig. 1b).

In Figs. 2a and 2d, the $ADPs$ in the three runs are displayed, but at the test point, and in Fig. 2c, the spatial ADP at $t=0.35$ s is displayed. These figures give insight into how the solution in EM is degraded compared to those in MNEF and MEF.

The parameter estimation processes for the diffusion coefficient ν, based on the MEF and MNEF models, are shown in Fig. 3a. One sees here that the estimated diffusion coefficient ν, based on the MEF model, converges very quickly to the true value $\nu=1$ m^2/s, whereas a long oscillation is required for the estimation process based on MNEF before convergence has been achieved. It means that the introduced EF well compensates an unmodeled error, existing in MNEF.

The estimated error field E_u and diffusion coefficient K_u are presented in Fig. 3b–c. From Fig. 3b it is seen that the error E_u decreases quickly as a function of time.

4.2. Test case 2: Experiment for advection equation

For the time period $[t_1,t_2]$, let us introduce the classical Burgers advection problem:

$$\begin{cases} \dfrac{\partial C}{\partial t}+a\dfrac{\partial C}{\partial x} = \eta\dfrac{\partial^2 C}{\partial x^2} & x\in[-0.5,0.5] \text{ and } t\in(t_1,t_2] \\ C = \operatorname{erfc}\left(-\dfrac{0.5+a\,t}{2\sqrt{\eta\,t}}\right) & \text{on } x=-0.5 \\ C = \operatorname{erfc}\left(\dfrac{0.5-a\,t}{2\sqrt{\eta\,t}}\right) & \text{on } x=0.5 \\ C(t_1) = C_0 \end{cases} \tag{37}$$

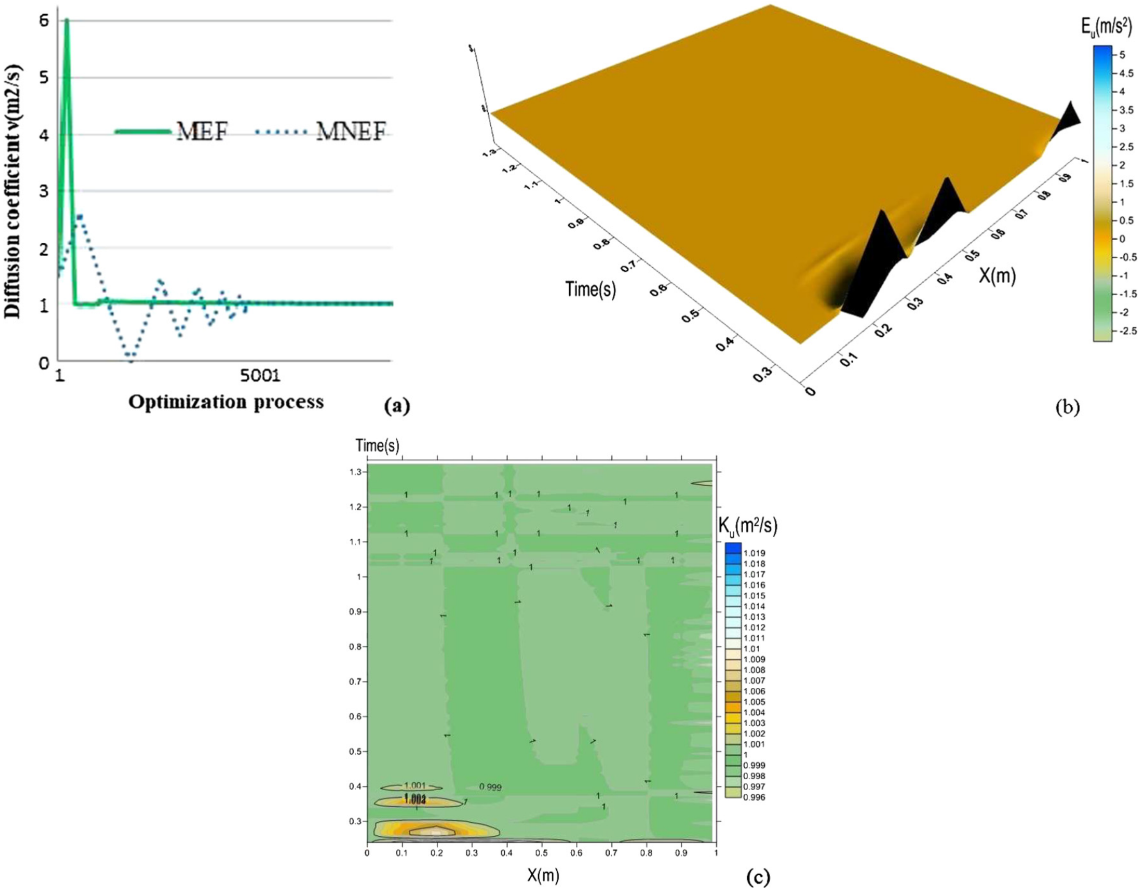

Fig. 3. Test case 1. Panel (a) displays the diffusion coefficient ν, estimated based on the models MEF and MNEF. It can be seen that the model MEF permits to identify quickly the coefficient ν, whereas with the model MNEF (without using EF), a long oscillation is required before the convergence is achieved. Panels (b)–(c): velocity error E_u and diffusion coefficient K_u in the spatio-temporal plane.

In the same fashion as in Eq. (37), but for the time period $[t_2, t_3]$, we will consider the forecast problem described by the following equations:

$$\begin{cases} \dfrac{\partial C}{\partial t} + a\dfrac{\partial C}{\partial x} = \eta \dfrac{\partial^2 C}{\partial x^2} & x \in [-0.5, 0.5] \text{ and } t \in (t_2, t_3] \\ C = \text{erfc}\left(-\dfrac{0.5 + at}{2\sqrt{\eta t}}\right) & \text{on } x = -0.5 \\ C = \text{erfc}\left(\dfrac{0.5 - at}{2\sqrt{\eta t}}\right) & \text{on } x = 0.5 \\ C(t_2) = \hat{C}_0 \end{cases} \tag{38}$$

The following data are given: $t_0 = 0.01$ s, $t_1 = 0.02$ s, $t_2 = 1.024$ s, $t_3 = 1.824$, $\Delta t = 0.0001$ s, $a = 1$ m/s. The measurements are given in three points with coordinates: $x = -0.3$ m, $x = -0.1$ m, $x = 0.4$ m. The test point is at $x = 0$.

We will consider the four models below.

– 1. Reference model (RM): The function

$$C(x,t) = \text{erfc}\left(\frac{x - at}{2\sqrt{\bar{\eta} t}}\right) \tag{39}$$

is the exact solution to the following equation system (see [3]):

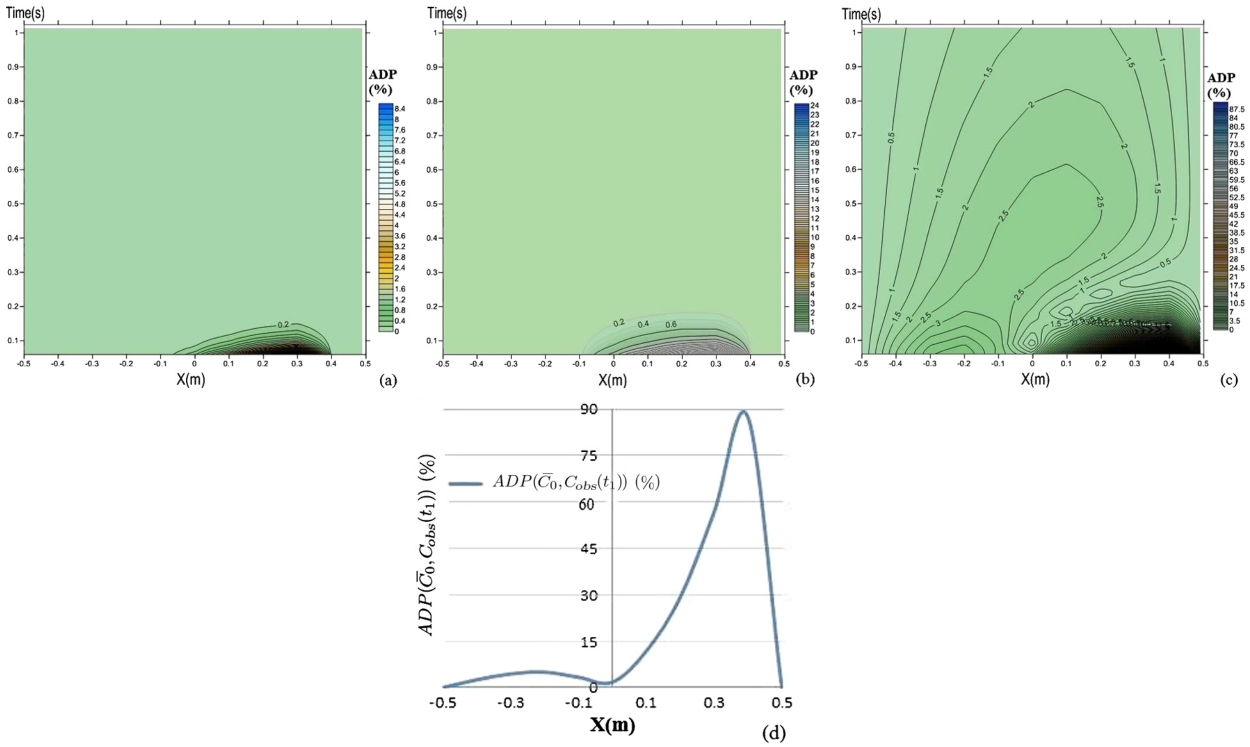

Fig. 4. Test case 2. Panels (a)–(c): spatio-temporal $ADP(concentration)$ between MEF and RM (a), MNEF and RM (b), EM and RM (c). Panel (d): spatial ADP between $\bar{C}_0$ and $C_{\text{obs}}(t_1)$.

$$\begin{cases} \dfrac{\partial C}{\partial t} + a\dfrac{\partial C}{\partial x} = \bar{\eta}\dfrac{\partial^2 C}{\partial x^2} & x \in [-0.5, 0.5] \text{ and } t \in [t_1, t_3] \\ C = \operatorname{erfc}\left(-\dfrac{0.5\,\operatorname{erfc}}{2\sqrt{\bar{\eta} t}}\right) \text{ on } x = -0.5 \\ C = \operatorname{erfc}\left(\dfrac{0.5 - at}{2\sqrt{\bar{\eta} t}}\right) \text{ on } x = 0.5 \\ C(t_1) = \operatorname{erfc}\left(\dfrac{x - at_1}{2\sqrt{\bar{\eta} t_1}}\right) \end{cases} \tag{40}$$

Using the formula (39) and s.t. $\bar{\eta} = 0.4$ m^2/s, we calculate the analytical solution to (40), which is called a *RM solution* (denoted by C_{obs}).

– 2. The erroneous model (EM) (i.e. without correction).
In this model, the value of the diffusion coefficient η and the initial condition C_0 are:
– $\eta = 0.6$ m^2/s;
– $C_0 = \bar{C}_0$, where $\bar{C}_0$ is defined by the following function:

$$\bar{C}_0 = \frac{1}{t_1 - t_0}\int_{t_0}^{t_1} \operatorname{erfc}\left(\frac{x - at}{2\sqrt{\eta t}}\right) \mathrm{d}t \tag{41}$$

The spatial $ADP(\bar{C}_0, C_{\text{obs}}(t_1))$ is shown in Fig. 4d. One sees that the maximum percentage level is about 90%. There is a significant difference between η and value $\bar{\eta}$.
The problem (37) is solved by s.t. η and C_0. The obtained solution is denoted by C_{EM}. The spatio-temporal $ADP(C_{\text{EM}}, C_{\text{obs}})$, over the time period $[t_1, t_2]$, is displayed in Fig. 4c. The maximum value of ADP is about 87%.
For the next time period $[t_2, t_3]$, the problem (38) is solved by s.t. $\hat{C}_0 = C_{\text{EM}}(t_2)$. For this time period, the $ADP(C^{\text{f}}_{\text{EM}}, C_{\text{obs}})$ at the test point is presented by the dashed red curve in Fig. 5d.

– 3. Introduce the model, including EF E_c (denoted as MEF).

Let us consider the following system of equations:

$$\begin{cases} \dfrac{\partial C}{\partial t}+a\dfrac{\partial C}{\partial x} = \eta\dfrac{\partial^2 C}{\partial x^2}+G_C\cdot E_C & x\in[-0.5,0.5] \text{ and } t\in(t_1,t_2] \\ \dfrac{\partial E_C}{\partial t} = \dfrac{\partial}{\partial x}\left(K_C(x)\dfrac{\partial E_C}{\partial x}\right) & x\in[-0.5,0.5] \text{ and } t\in(t_1,t_2] \\ C = \operatorname{erfc}\left(-\dfrac{0.5\,\operatorname{erfc}}{2\sqrt{\eta t}}\right) & \text{on } x=-0.5 \\ C = \operatorname{erfc}\left(\dfrac{0.5-at}{2\sqrt{\eta t}}\right) & \text{on } x=0.5 \\ E_C = 0 & \text{on } x=-0.5 \\ E_C = 0 & \text{on } x=0.5 \\ C(t_1) = C_0 \\ E_C(t_1) = V_C \end{cases} \tag{42}$$

The problem is to adjust the initial condition C_0, V_C and the diffusion coefficients η, K_C to produce a solution C that is as close as possible to the RM solution C_{obs}. For this purpose, let us introduce the cost function:

$$\bar{\Im}(C_0,\eta,V_C,K_C)=\frac{1}{2}\parallel G_C C-C_{\text{obs}}\parallel^2_{Y_{C_{\text{obs}}}}+\frac{1}{2}\parallel C_0-\bar{C}_0\parallel^2_{L_2(X_C)}+\frac{1}{2}\parallel \eta-\eta_0\parallel^2+\frac{1}{2}\int_{t_1}^{t_2}\parallel E_C\parallel^2_{L_2(\wp_C)}\,\mathrm{d}t$$
$$+\frac{1}{2}\parallel V_C-V_{C,0}\parallel^2_{L_2(\wp_C)}+\frac{1}{2}\parallel K_C-K_{C,0}\parallel^2_{Y_p} \tag{43}$$

Here the variables $\bar{C}_0$, η_0, $K_{C,0}$ and $V_{C,0}$ are given a priori.
The optimization problem is to minimize the cost function (43) to find the optimal values ν^*, K_C^*, C_0^* and V_C^* s.t. the system of equations (42), i.e.

$$\begin{cases} \dfrac{\partial C}{\partial t}+a\dfrac{\partial C}{\partial x} = \eta\dfrac{\partial^2 C}{\partial x^2}+G_C\cdot E_C & x\in[-0.5,0.5] \text{ and } t\in(t_1,t_2] \\ \dfrac{\partial E_C}{\partial t} = \dfrac{\partial}{\partial x}\left(K_C(x)\dfrac{\partial E_C}{\partial x}\right) & x\in[-0.5,0.5] \text{ and } t\in(t_1,t_2] \\ C = \operatorname{erfc}\left(-\dfrac{0.5\,\operatorname{erfc}}{2\sqrt{\eta t}}\right) & \text{on } x=-0.5 \\ C = \operatorname{erfc}\left(\dfrac{0.5-at}{2\sqrt{\eta t}}\right) & \text{on } x=0.5 \\ E_C = 0 & \text{on } x=-0.5 \\ E_C = 0 & \text{on } x=0.5 \\ C(t_1) = C_0(x) \\ E_C(t_1) = V_C \\ \bar{\Im}(C_0^*,\eta^*,V_C^*,K_C^*) = \operatorname{Arg}\min\limits_{C_0,\eta,V_C,K_C}\bar{\Im}(C_0,\eta,V_C,K_C) \end{cases} \tag{44}$$

The gradient of the cost function $\bar{\Im}(C_0,\eta,V_C,K_C)$ is:

$$\nabla\bar{\Im}(C_0,\eta,V_C,K_C)=\left(\bar{\Im}'_{C_0},\bar{\Im}'_{\eta},\bar{\Im}'_{V_C},\bar{\Im}'_{K_C}\right) \tag{45}$$

where $\bar{\Im}'_{C_0}$, $\bar{\Im}'_{\eta}$, $\bar{\Im}'_{V_C}$ and $\bar{\Im}'_{K_C}$ are defined by

$$\begin{cases} \bar{\Im}'_{C_0} = C_0-\bar{C}_0-\hat{P}_C(t_1) \\ \bar{\Im}'_{\eta} = \eta-\eta_0+\displaystyle\int_{t_1}^{t_2}\left(\frac{\partial C}{\partial x},\frac{\partial\hat{P}_C}{\partial x}\right)\mathrm{d}t \\ \bar{\Im}'_{V_C} = V_C-V_{C,0}-\hat{Q}_C(t_1) \\ \bar{\Im}'_{K_C} = K_C-K_{C,0}+\displaystyle\int_{t_1}^{t_2}\frac{\partial E_C}{\partial x}\frac{\partial\hat{Q}_C}{\partial x}\,\mathrm{d}t \end{cases} \tag{46}$$

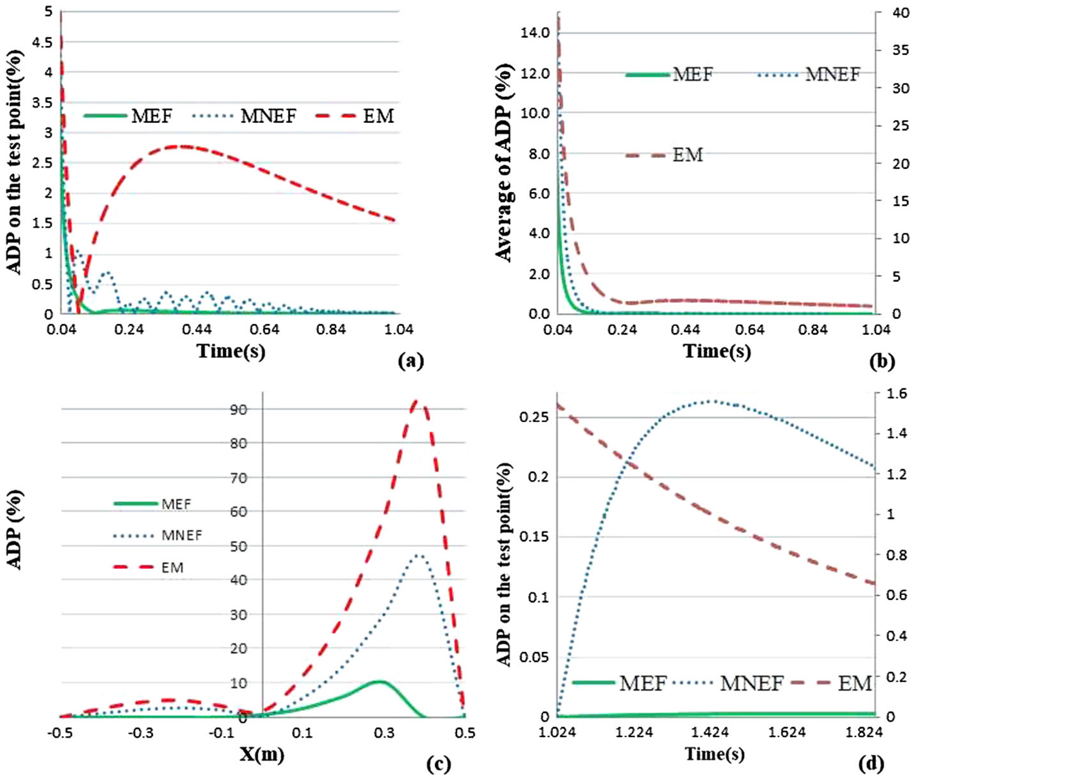

Fig. 5. Test case 2. Panel (a) shows the $ADP(concentration)$ between MEF, MNEF, EM, and RM at the test point. Panel (b) displays the time average of the curves in (a). Let us mention that the ordinate values of MEF and MNEF are projected onto the left vertical axis, whereas for EM they are projected onto the right vertical axis. Panel (c) displays the spatial $ADP(concentration)$ between MEF, MNEF, ME, and RM at time $t = 0.06$ s. Panel (d) is the same as panel (a), but for the forecasting time period $[t_2, t_3]$. The values of MEF and MNEF are projected on the left vertical axis and those of EM on the right vertical axis.

The variables $\hat{P}_C$ and $\hat{Q}_C$ are the solutions to the following system of equations:

$$\begin{cases} \dfrac{\partial \hat{P}_C}{\partial t} = -a\dfrac{\partial \hat{P}_C}{\partial x} - \eta\dfrac{\partial^2 \hat{P}_C}{\partial x^2} + G_C^{\mathsf{T}}\cdot(G_C C - C_{\text{obs}}), \; x \in [-0.5, 0.5], t \in [t_1, t_2) \\ \hat{P}_C = 0 \quad \text{on } x = -0.5 \\ \hat{P}_C = 0 \quad \text{on } x = 0.5 \\ \hat{P}_C(t_2) = 0 \end{cases} \tag{47}$$

$$\begin{cases} \dfrac{\partial \hat{Q}_C}{\partial t} = \dfrac{\partial}{\partial x}\left(K_C(x)\dfrac{\partial \hat{Q}_C}{\partial x}\right) - G_C^{\mathsf{T}}\cdot\hat{P}_C + E_C \qquad x \in [-0.5, 0.5] \text{ and } t \in [t_1, t_2) \\ \hat{Q}_C = 0 \quad \text{on } x = -0.5 \\ \hat{Q}_C = 0 \quad \text{on } x = 0.5 \\ \hat{Q}_C(t_2) = 0 \end{cases} \tag{48}$$

The problem (44) is solved by s.t. $\eta_0 = 1.5\,\bar{\eta} = 0.6$ m^2/s, $K_{C,0} = 1$ m^2/s, the parameter $\bar{C}_0$ is defined by (41), and $V_{C,0}$ is chosen by

$$V_{C,0} = \begin{cases} C_{\text{obs}}(t_1) - \bar{C}_0 \text{ on measurement points} \\ 0 \text{ on no-measurement points} \end{cases} \tag{49}$$

Applying the BFGS method (see [2], [10]) with $\nabla\bar{\Im}(C_0, \eta, V_C, K_C)$, defined by (45), yields the optimal values C_0^*, η^*, V_C^*, K_C^*.

The system of Eqs. (42) is solved next s.t. $C_0 = C_0^*$ and $\eta = \eta^*_{\text{MEF}}$, $V_C = V_C^*$, $K_C = K_C^*$. The obtained solution is denoted by C_{MEF}. For the time interval $[t_1, t_2]$, the $ADP(C_{\text{MEF}}, C_{\text{obs}})$ is shown in Fig. 4a. One sees that the maximum value is about 8.4%.

For the next time period $[t_2, t_3]$, the problem (38) is solved by s.t. $\eta = \eta^*_{\text{MEF}} = 0.4$ m^2/s and $\hat{C}_0 = C_{\text{MEF}}(t_2)$. The solution is denoted by $C^{\text{f}}_{\text{MEF}}$. For this time period, the $ADP(C^{\text{f}}_{\text{MEF}}, C_{\text{obs}})$ is presented by the grid green curve of Fig. 5d.

– 4. The model, not including EF E_C, is denoted by "MNEF". Consider the problem (37). The optimization problem is to identify the initial condition C_0 and the diffusion coefficient η to produce a solution C that is as close as possible to C_{obs}. For this purpose, we introduce the cost function:

$$\Im(C_0, \eta) = \| G_C C - C_{\text{obs}} \|^2_{Y_{C_{\text{obs}}}} + \frac{1}{2} \| C_0 - \bar{C}_0 \|^2_{L_2(X_C)} + \frac{1}{2} \| \eta - \eta_0 \|^2 \tag{50}$$

Here the values $\bar{C}_0$ and η_0 are given.
Then the corresponding optimization problem is to find the optimal diffusion values ν^* and the initial conditions C_0^* of the system of equations (37) and is formulated as

$$\begin{cases} \dfrac{\partial C}{\partial t} + a \dfrac{\partial C}{\partial x} = \eta \dfrac{\partial^2 C}{\partial x^2} & x \in [-0.5, 0.5] \text{ and } t \in (t_1, t_2) \\ C = \text{erfc}\left(-\dfrac{0.5\,\text{erfc}}{2\sqrt{\eta t}}\right) & \text{on } x = -0.5 \\ C = \text{erfc}\left(\dfrac{0.5 - a t}{2\sqrt{\eta t}}\right) & \text{on } x = 0.5 \\ C(t_1) = C_0 \\ \Im(C_0^*, \eta^*) = \text{Arg}\min\limits_{C_0, \eta} \Im(C_0, \eta) \end{cases} \tag{51}$$

The gradient of the cost function $\Im(C_0, \eta)$ is:

$$\nabla \Im(C_0, \eta) = \left(\Im'_{C_0}, \Im'_\eta\right) \tag{52}$$

Here, $\Im'_{C_0}, \Im'_\eta$ are defined by the following formula:

$$\begin{cases} \Im'_{C_0} = C_0 - \bar{C}_0 - \hat{P}_C(t_1) \\ \Im'_\eta = \eta - \eta_0 + \displaystyle\int_{t_1}^{t_2} \left(\frac{\partial C}{\partial x}, \frac{\partial \hat{P}_C}{\partial x}\right) \mathrm{d}t \end{cases} \tag{53}$$

where $\hat{P}_C$ is the solution of the system of Eqs. (47).
The problem (51) is solved with $\eta_0 = 1.5\,\bar{\eta} = 0.6$ m^2/s and $\bar{C}_0$ defined by formula (41). Using $\nabla\Im(C_0, \eta)$, defined by (52), we can find the optimal values C_0^*, η^* by solving the optimization problem (51) with the BFGS method (see [2], [10]). For further convenience, η^* is denoted by η^*_{MNEF}. The system of Eqs. (37) is solved by s.t. $C_0 = C_0^*$ and $\eta = \eta^*_{\text{MNEF}}$. The obtained solution is denoted by C_{MNEF}. For the time period $[t_1, t_2]$, the $ADP(C_{\text{MNEF}}, C_{\text{obs}})$ is displayed in Fig. 4b. One sees that the maximum value of ADP is about 24%. For the next time period $[t_2, t_3]$, we compute the forecast by solving (38) s.t. $\eta = \eta^*_{\text{MNEF}} = 0.44$ m^2/s and $\hat{C}_0 = C_{\text{MNEF}}(t_2)$. Its solution is denoted by $C^{\text{f}}_{\text{MNEF}}$. The curve for $ADP(C^{\text{f}}_{\text{MNEF}}, C_{\text{obs}})$ is labelled as MNEF in Fig. 5d.

We want to emphasize that all the figures in Fig. 5 confirm the important role played by the VDA algorithm as a tool for improving the resolution of the numerical model (compare the error levels in MNEF and in EM). Moreover, the introduction of EF into the model equation well compensates a discrepancy between the model and the true state of the system, which has a really positive impact on the decrease of the estimation error (compare the two curves MEF and MNEF).

The typical optimization processes for estimating the diffusion coefficient η, with and without EF, are shown in Fig. 6a. One sees that the correction process with EF (curve MEF) converges much more quickly compared with the case of MNEF. The estimated error field E_C is presented in Fig. 6b. One sees here that there are strong changes located around the three measurement points.

4.3. Test case 3: simulation experiment for Burgers' pollution model

In this section, we will consider the problems (1)–(4), (13), (14), (19) in which the boundary conditions on $x = L$ are given as follows:

$$\begin{cases} \dfrac{\partial U}{\partial x} = 0 & \text{on } x = L \\ \dfrac{\partial C}{\partial x} = 0 & \text{on } x = L \end{cases} \tag{54}$$

The flow is computed under the conditions $L_0 = 0$, $L = 1$ m, time step $\Delta t = 0.0001$ s, $U_{\text{in}} = 0.5$ m/s, $t_1 = 0$, $t_2 = 0.5$ s, $t_3 = 3.5$ s, $C_{\text{in}} = 5$ mg/l. We will suppose that the measurements are available at three spatial points: $x = 0.2$ m, $x = 0.4$ m, $x = 0.9$ m. The performance is tested at the point (called a test point) $x = 0.8$ m.

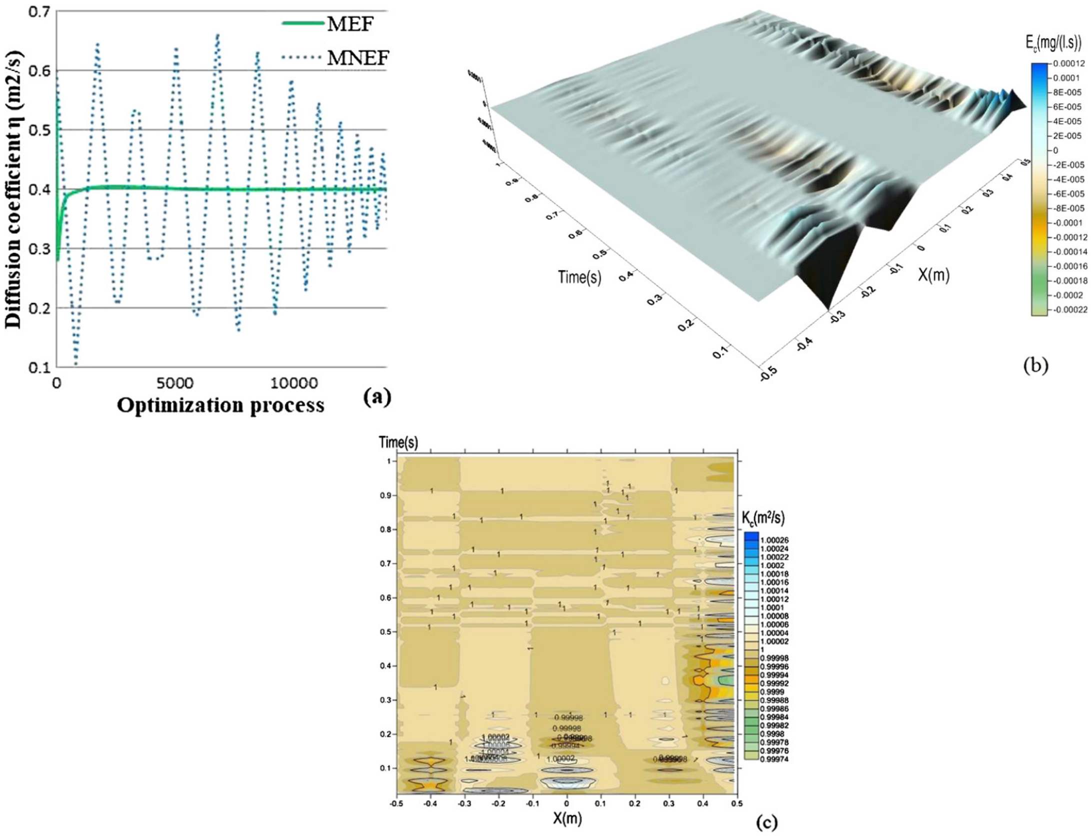

Fig. 6. Test case 2. Panel (a): the curves MEF and MNEF show the diffusion coefficient η, estimated based on the MEF and MNEF models, respectively. Panel (b): error for the concentration coefficient E_C in the spatio-temporal plane. Panel (c): The diffusion coefficient K_C in the spatio-temporal plane.

The experiment is performed in the framework of a "twin experiment" (see [7], [15]).

- 1. The reference model (RM).
For the time period $[t_1, t_2]$, solve the Eqs. (13), (14) s.t. $\eta = \bar{\eta} = 0.4$ m^2/s, $\nu = \bar{\nu} = 1$ m^2/s and the initial condition $U_{\text{obs}}(t_1)$, $C_{\text{obs}}(t_1)$ (see the grid red curves in Fig. 7a and 7b). The solution is the couple (U_{obs}, C_{obs}) (considered as a reference). Next we compute the forecast for the time period $[t_2, t_3]$ by solving (19) s.t. $\hat{U}_0 = U_{\text{obs}}(t_2)$ and $\hat{C}_0 = C_{\text{obs}}(t_2)$.
- 2. The erroneous model (EM)
For the time period $[t_1, t_2]$, the Eqs. (13), (14) are solved with diffusion coefficients $\nu = 1.5\,\bar{\nu} = 1.5$ m^2/s, $\eta = 1.5\,\bar{\eta} = 0.6$ m^2/s and the initial condition values $U_0 = \bar{U}_0$, $C_0 = \bar{C}_0$. Here $\bar{U}_0$, $\bar{C}_0$ are obtained by a "twin-experiment" (see [7]) and they are displayed in Figs. 7a, 7b. The $ADP(\bar{U}_0, U_{\text{obs}}(t_1))$ and $ADP(\bar{C}_0, C_{\text{obs}}(t_1))$ are presented in Figs. 7c and 7d, respectively. One sees there that the maximum percentage levels are about 12% and 10%, respectively. The rates between ν, η and $\bar{\nu}$, $\bar{\eta}$ are equal to 1.5.
The velocities and concentration of this model are denoted by U_{EM} and C_{EM}. The $ADP(U_{\text{EM}}, U_{\text{obs}})$ and $ADP(C_{\text{EM}}, C_{\text{obs}})$ are shown in Figs. 10c and Fig. 11c, respectively. Next the forecast solution $(U^{\text{f}}_{\text{EM}}, C^{\text{f}}_{\text{EM}})$ is computed by solving the problem (19) s.t. the initial condition $\hat{U}_0 = U_{\text{EM}}(t_2)$ and $\hat{C}_0 = C_{\text{EM}}(t_2)$ for the next time period $[t_2, t_3]$. The $ADP(C^{\text{f}}_{\text{EM}}, C_{\text{obs}})$ and $ADP(U^{\text{f}}_{\text{EM}}, U_{\text{obs}})$ at the test point are presented by the dash red curves in Figs. 8d and 9d.
- 3. The model including EF E_u, E_C (MEF):
By the way shown in subsection 2.1, the optimization problem (6) with the boundary conditions (54) is solved by s.t. $\nu_0 = 1.5$ m^2/s, $\eta_0 = 0.6$ m^2/s, $K_{u,0} = 1$ m^2/s, $K_{C,0} = 1$ m^2/s, and $\bar{U}_0$, $\bar{C}_0$ (shown by the dash blue curves of Figs. 7a and 7b), $V_{u,0}$, $V_{C,0}$ (defined by (32), (49)). The obtained optimal values are U^*_0, C^*_0, V^*_u, V^*_C, η^*, ν^*, K^*_u, K^*_C. For further use, we denote ν^*, η^* by ν^*_{MEF} and η^*_{MEF}, respectively. The system of Eqs. (1)–(4) is then solved by s.t. $U_0 = U^*_0$, $C_0 = C^*_0$, $\nu = \nu^*_{\text{MEF}}$ and $\eta = \eta^*_{\text{MEF}}$, $V_u = V^*_u$, $V_C = V^*_C$, $K_u = K^*_u$, $K_C = K^*_C$. The obtained solutions are denoted by U_{MEF}, C_{MEF}. The $ADP(C_{\text{MEF}}, C_{\text{obs}})$, $ADP(U_{\text{MEF}}, U_{\text{obs}})$ are shown in Figs. 10a and 11a, respectively. For the next time period $t \in [t_2, t_3]$, the problem (19) is solved by s.t. $\eta = \eta^*_{\text{MEF}} = 0.4$ m^2/s, $\nu = \nu^*_{\text{MEF}} = 1.00001$ m^2/s and $\hat{U}_0 = U\text{MEF}(t_2)$, $\hat{C}_0 = C_{\text{MEF}}(t_2)$. Its solution is denoted by $(U^{\text{f}}_{\text{MEF}}, C^{\text{f}}_{\text{MEF}})$. The curves for $ADP(U^{\text{f}}_{\text{MEF}}, U_{\text{obs}})$, $ADP(C^{\text{f}}_{\text{MEF}}, C_{\text{obs}})$ are presented by the grid green curves in Figs. 8d and 9d.

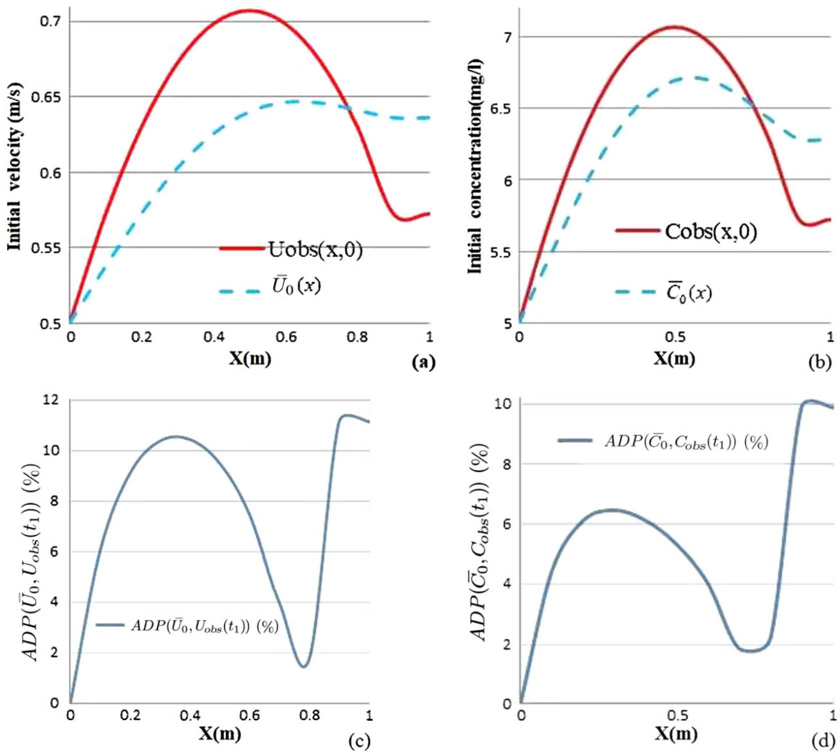

Fig. 7. Test case 3. Panel (a): the initial true velocity $U_{\text{obs}}(t_1)$ used in RM and $\bar{U}_0$ the guess (velocity) used in EM. Panel (b): the initial true concentrations $C_{\text{obs}}(t_1)$ used in RM and $\bar{C}_0$ the guess for concentration used in EM. Panel (c): ADP between $\bar{U}_0$ and $U_{\text{obs}}(t_1)$. Panel (d): ADP between $\bar{C}_0$ and $C_{\text{obs}}(t_1)$.

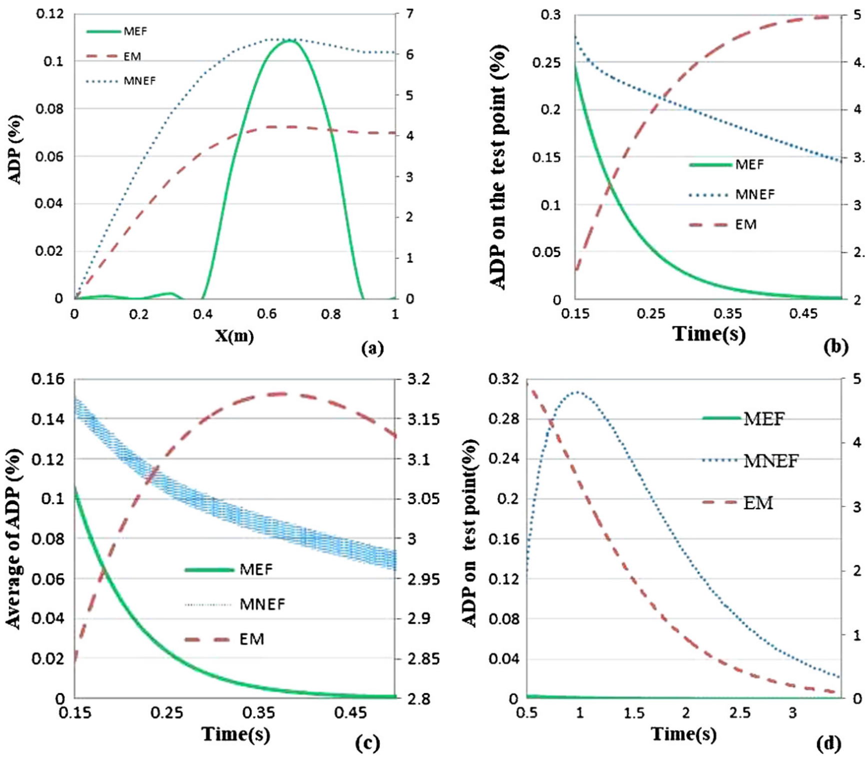

Fig. 8. Test case 3. Panel (a): spatial $ADP(concentration)$ between three runs MEF, MNEF, EM, and RM at the moment $t = 0.232$ s. The values of EM are projected onto the right vertical axis. Panel (b): the same as in (a), but at the test point and for the period $[0.15 - 0.5$ s$]$. Panel (c): time-average $ADP(concentration)$ between MEF, MNEF, EM, and RM. The values of the curve EM are projected onto the right vertical axis. Panel (d): the same as in (b), but at the test point and for the time period $[t_2, t_3]$.

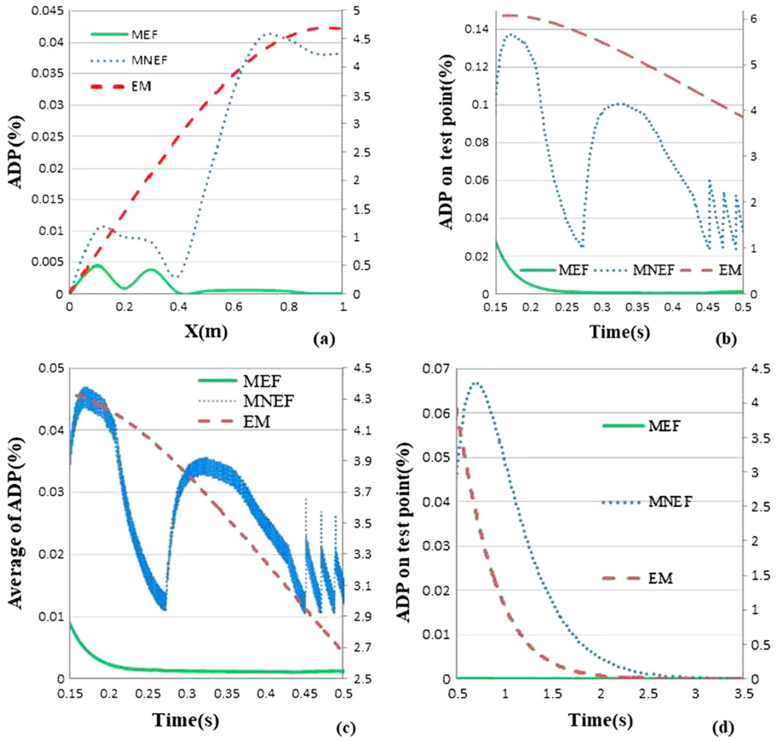

Fig. 9. Test case 3. Panel (a): the curves MEF, MNEF, and EM show $ADP(velocity)$ between three runs MEF, MNEF, EM, and RM at the test point and at $t = 0.0034$ s. The values of the curve EM are projected onto the right vertical axis. Panel (b): the same curves as in (a) but over the time period $t \in [0.15\,\text{s}, 0.5\,\text{s}]$. Panel (c): time-averaged $ADP(velocity)$ of the curves in (b) for the time period $t \in [0.15\,\text{s}, 0.5\,\text{s}]$. Panel (d): The same as in (b), but for the forecasting time period $[t_2, t_3]$.

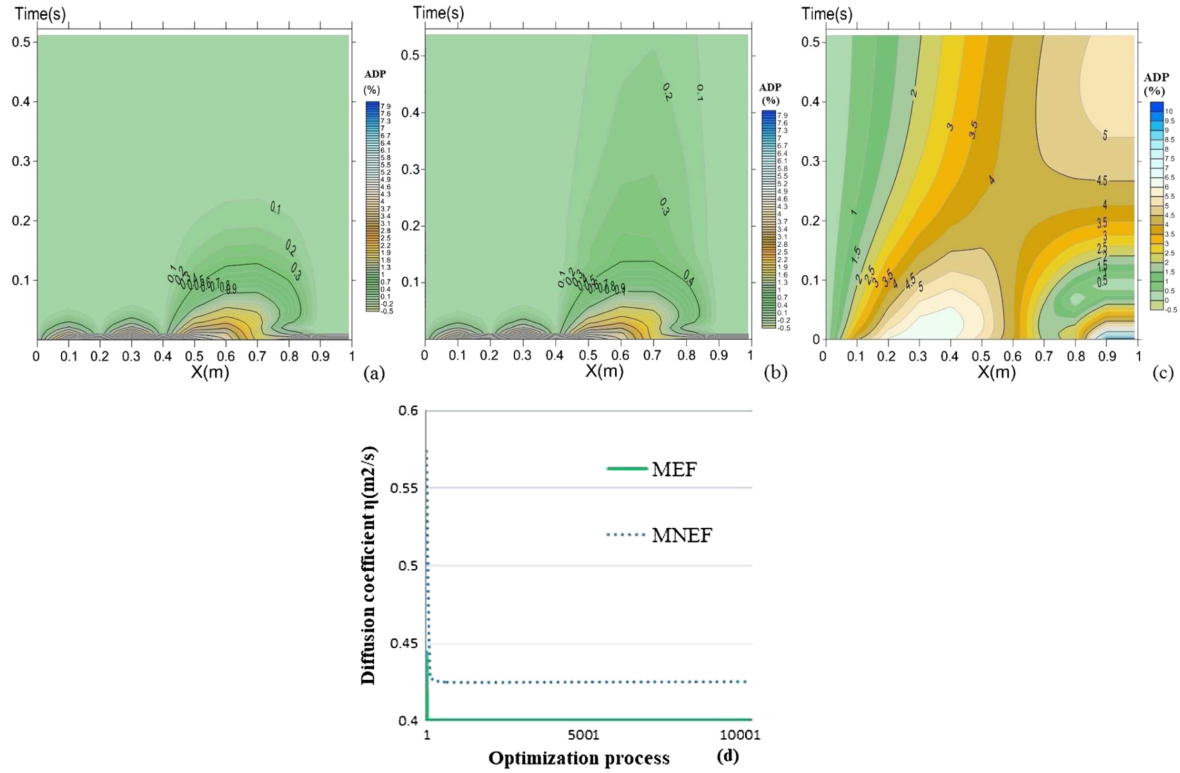

Fig. 10. Test case 3. Panel (a): spatio-temporal $ADP(concentration)$ between MEF and RM. Panel (b): the same as in (a), but between MNEF and RM. Panel (c): the same as in (a), but between EM and RM. Panel (d): convergence of the estimated diffusion coefficient η based on MEF and MNEF models.

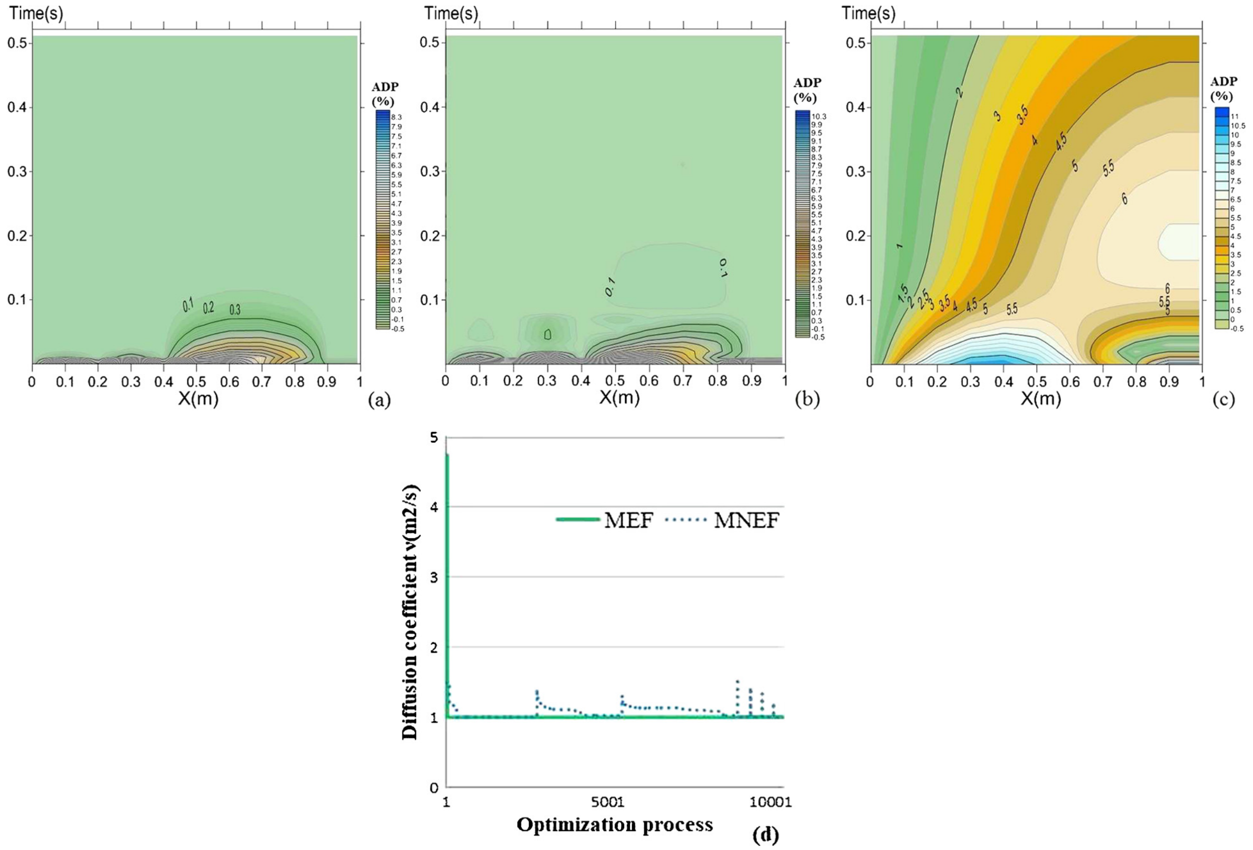

Fig. 11. Test case 3. Panels (a)–(c): the same as in Fig. 10, but for the $ADP(velocity)$: c of the estimated diffusion coefficient ν based on the MEF and MNEF models.

In Figs. 12(a), 12(b) we show the spatio-temporal estimates for the velocity EF E_u and the concentration EF E_C. As to the estimated diffusion coefficients K_u (c) and K_C (d), their estimates are displayed in Figs. 12(c) and 12(d).

– 4. The model not including EF E_u, E_C (MNEF).
As in subsection 2.2, the problem (16) with boundary conditions (54) is solved by s.t. (i) $\nu_0 = 1.5\ \text{m}^2/\text{s}$, $\eta_0 = 0.6\ \text{m}^2/\text{s}$; (ii) $\bar{U}_0$ and $\bar{C}_0$ (see Figs. 7a, 7b). The obtained optimal parameters are U_0^*, C_0^* and ν^*, η^*. We denote by ν^*_{MNEF} and η^*_{MNEF} the optimal values ν^*, η^*. The system of Eqs. (13), (14) is solved by s.t. $U_0 = U_0^*$, $C_0 = C_0^*$, $\nu = \nu^*_{\text{MNEF}}$ and $\eta = \eta^*_{\text{MNEF}}$. Its solution is denoted by $(U_{\text{MNEF}}, C_{\text{MNEF}})$. The curves for $ADP(C_{\text{MNEF}}, C_{\text{obs}})$, $ADP(U_{\text{MNEF}}, U_{\text{obs}})$ are displayed in Figs. 10b, 11b respectively. For the next time period $t \in [t_2, t_3]$, the problem (19) is solved by s.t. $\eta = \eta^*_{\text{MNEF}} = 0.42\ \text{m}^2/\text{s}$, $\nu = \nu^*_{\text{MNEF}} = 1.01\ \text{m}^2/\text{s}$ and $\hat{U}_0 = U_{\text{MNEF}}(t_2)$, $\hat{C}_0 = C_{\text{MNEF}}(t_2)$. Its solution is denoted by $(U^{\text{f}}_{\text{MNEF}}, C^{\text{f}}_{\text{MNEF}})$. The dotted blue curves for $ADP(C^{\text{f}}_{\text{MNEF}}, C^{\text{f}}_{\text{obs}})$, $ADP(U^{\text{f}}_{\text{MNEF}}, U^{\text{f}}_{\text{obs}})$ on the test point are presented in Figs. 8d and 9d.

5. Conclusion

This paper presents the results of a comparative study on the impact of an error function on the estimation of a solution for the transport of pollution substances based on Burgers' equation. The classical approach to improve the system solution based on the VDA method is to minimize the cost function by tuning the initial condition and the diffusion coefficient. The objective is the comparison of the performance of the classical approach with that based on the EF method. The originality of the EF approach resides in an introduction of the error functions (EFs) E_u, E_c into Burgers' equations to compensate for the model error. A new variational problem is formulated on the basis of the extended system of equations with a new vector of control. To see the effect of the introduced EF on the improvement of the estimated solution, three test cases have been experimented, in which three models are systematically used: EM, MEF, and MNEF.

The numerical experiments show that:

– the $ADP(U, U_{\text{obs}})$, $ADP(C, C_{\text{obs}})$ of model MEF are much lower than the ones of the other models EM and MNEF;
– in the optimization processes, the diffusion coefficients ν and η of model MEF come much closer and faster to the proposed values than the ones of model MNEF.

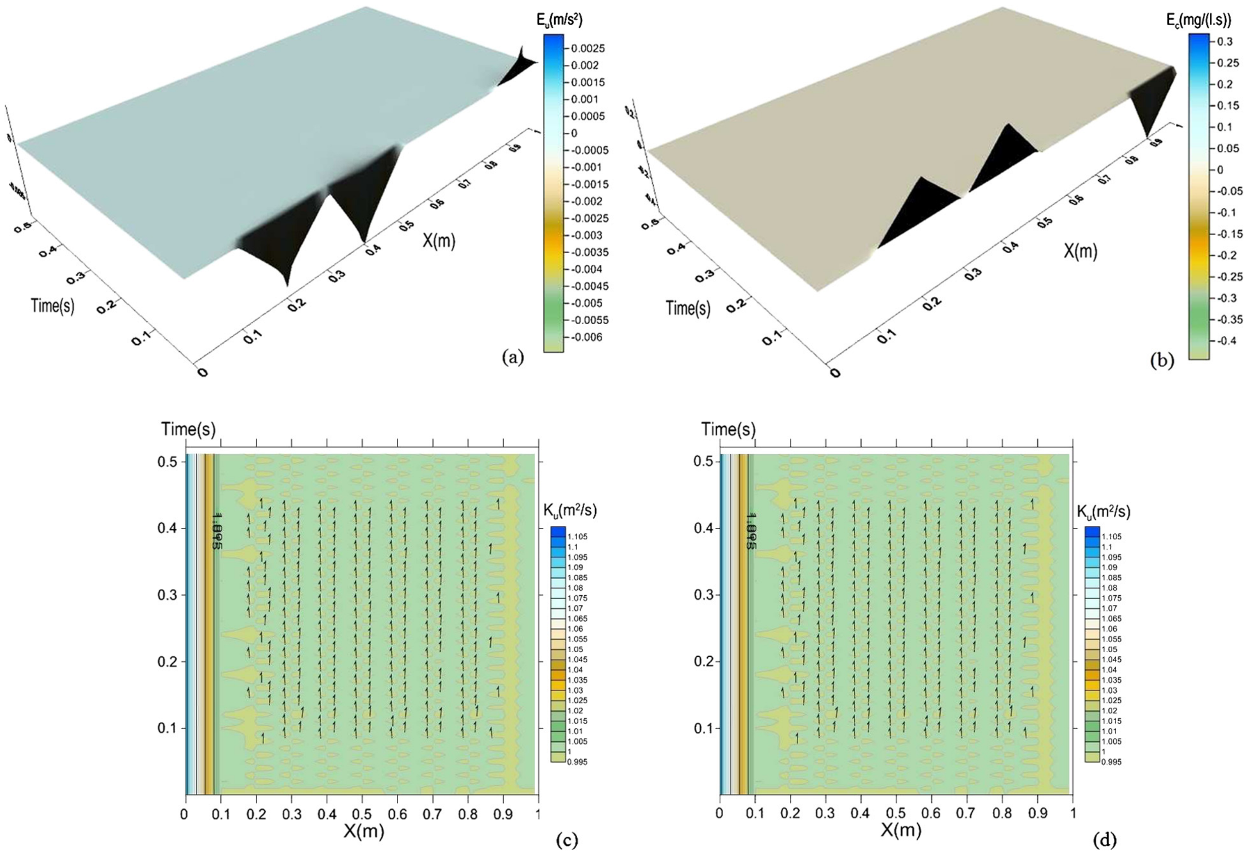

Fig. 12. Test case 3. Spatio-temporal estimates for: velocity EF E_u (a); concentration EF E_C (b); diffusion coefficient K_u (c); diffusion coefficient K_C (d).

It follows that the EF approach overperforms compared to the classical approach and leads to a better forecast of substance contents and water quality.

It must be mentioned that the proper choice of EF plays a major role in guaranteeing a good performance of the proposed EF approach. Finding a relatively general method for an appropriate choice of EFs for different dynamical systems is an important and not easy task, and is left for a future study.

Based on the successes of the presented method for solving the 1D problem, a study on a 2D water pollution is underway, and we do hope to report the results on a 2D problem in a near future.

In order to have a good correction method, in this paper the EFs E_u and E_C, satisfying the systems of Eqs. (3)–(4), are introduced in Eqs. (1), (2). One natural question that arises then is to compare the impact of the introduced EF with the others to see its advantages, if they exist, over the other EF structures in solving DA problems.

Appendix

For the simplicity of the presentation, suppose that the true system is described by

$$\phi^*(t+1) = \Phi(\phi^*(t)), \phi^*(0) = u^*, t = 0, ..., T \tag{55}$$

where $\Phi(.) : R^n \to R^n$. The observation $z(t) \in R^p$ is given by

$$z(t+1) = H\phi^*(t+1) + v(t+1), t = 0, ..., T \tag{56}$$

where $H : R^p \to R^n$, $v(t)$ represents the observation error.

Introduce the numerical model

$$\phi(t+1) = \Phi(\phi(t)), \phi(0) = u, t = 0, ..., T \tag{57}$$

It is seen that the solution $\phi^*(t)$ is well defined up to the initial condition u. From (57), by expressing $\phi(t)$ as a function of $\phi(0)$, the classical VDA tries to seek $\theta := u$ from the optimization problem

$$\hat{u} = \arg\min_{\theta\in\Theta} J(\theta)$$

$$J(\theta) = \frac{1}{2}||\theta - u_b||^2_{M^{-1}} + \frac{1}{2}\sum_{t=1}^{\mathsf{T}}||z - H\phi(t)||^2_{R^{-1}} \tag{58}$$

where u_b represents the a priori knowledge of the initial state, R is the covariance matrix of v, M is the background error covariance matrix (ECM). Particularly important is the specification of the background ECM. For more details, see [8], [9], [18].

In practice, however, we do not know exactly Φ and instead of Φ we are given only F. The numerical model used for assimilation should be

$$x(t+1) = F(x(t)), x(0) = v, t = 0, ..., T \tag{59}$$

where $F(.): R^n \to R^n$. To compensate for the error resulting from the difference between Φ and F (and other sources of error like numerical error, discretization error...), instead of (59), we introduce the new model

$$x(t+1) = F(x(t)) + f(t), x(0) = \mu, t = 0, ..., T \tag{60}$$

where $f(t)$ represents the model error (ME). Thus, by assuming $f \neq 0$, there is an interest to consider f as an unknown to be estimated. For example, one can assume that f is a solution to some equation, i.e.

$$f(t+1) = \Psi(f(t)), t \in (0, T), f(0) = \psi \tag{61}$$

A corresponding cost function is introduced for the extended system written for the extended state $(x^{\mathsf{T}}(t), f^{\mathsf{T}}(t))^{\mathsf{T}}$ and with $\theta := (u^{\mathsf{T}}, \psi^{\mathsf{T}})^{\mathsf{T}}$ as a control vector.

Comment A1. MEs are coming from different sources, some of which constant, others periodic or flow dependent. ME may also come from discretization, numerical errors... The simplest approximation is to consider the ME as constant. We have then $\Psi = I$ – the identity matrix. Equation (59) s.t. $\Psi \neq I$ corresponds to the situation when the ME follows a predefined time dependency. Markov chains, Fourier series expansions or neuron networks, etc., are other potential choices.

Comment A2.

One important question concerns the choice of the background vector $\theta_b = u_b$. Its choice depends on a priori knowledge we have on the initial system state $\phi(0)$ and of ME (ensemble mean, climatology...).

Acknowledgements

We thank the anonymous reviewers for their careful reading of our manuscript and their insightful comments and suggestions.

The authors gratefully acknowledge the financial support from the NAFOSTED 107.03-2015.31 funds.

References

[1] J. Biazar, H. Aminikhah, Exact and numerical solutions for non-linear Burgers' equation by VIM, Math. Comput. Model. 49 (2009) 1394–1400, https://doi.org/10.1016/j.mcm.2008.12.00.
[2] J.F. Bonnans, J.Ch. Gilbert, C. Lemaráchal, C.A. Sagastizábal, Numerical Optimization, Theoretical and Numerical Aspects, second edition, Springer, 2006, p. 491.
[3] C. Hirsch, Numerical Computation of Internal and External Flows, vol. 2, 1994, p. 690.
[4] D. Furbish, M.Y. Hussaini, F.-X. Le Dimet, P. Ngnepieba, Y. Wu, On discretization error and its control in variational data assimilation, Tellus 60A (2008) 979–991, https://doi.org/10.1111/j.1600-0870.2008.00358.x.
[5] F.-X.L. Dimet, P. Ngnepieba, V. Shutyaev, On error analysis in data assimilation problems, Russ. J. Numer. Anal. Math. Model. 17 (1) (2002) 71–98, https://doi.org/10.1515/rnam-2002-0105.
[6] F.-X. Le Dimet, V. Shutyaev, On deterministic error analysis in variational data assimilation, Nonlinear Process. Geophys. 12 (4) (2005) 481–490, https://doi.org/10.5194/npg-12-481, 2005.
[7] F.-X. Le Dimet, V.P. Shutyaev, T.H. Tran, General sensitivity analysis in data assimilation, Russ. J. Numer. Anal. Math. Model. 29 (2) (2014) 107–127, https://doi.org/10.1515/rnam-2014-0009.
[8] I.Y. Gejadze, F.-X. Le Dimet, V. Shutyaev, On optimal solution error covariances in variational data assimilation problems, J. Comput. Phys. 229 (6) (2010) 2159–2178, https://doi.org/10.1016/j.jcp.2009.11.028.
[9] I.Y. Gejadze, G.J.M. Copeland, F.-X. Le Dimet, V. Shutyaev, Computation of the analysis error covariance in variational data assimilation problems with nonlinear dynamics, J. Comput. Phys. 230 (22) (2011) 7923–7943, https://doi.org/10.1016/j.jcp.2011.03.039.
[10] L.I.C. Gilbert, Some numerical experiments with variable-storage quasi-Newton algorithm, Math. Program. 45 (3) (1989) 407–435.
[11] J.-L. Lions, Contrôle optimal de systèmes gouvernés par des équations aux dérivées partielles, Dunod, Paris, 1968, p. 426.
[12] J.L. Lions, Contrôlabilité exacte perturbations et stabilisation de systèmes distribués, Masson, Paris, 1988, p. 296.
[13] G.I. Marchuk, V.I. Agoshkov, V.P. Shutyaev, Adjoint Equations and Perturbation Algorithms in Nonlinear Problems, CRC Press, 1996, p. 288.
[14] S.K. Park, L. Xu, Data Assimilation for Atmospheric, Oceanic and Hydrologic Applications, vol. III, Springer, ISBN 978-3-319-43415-5, 2017, p. 480.
[15] T.T. Ha, P.D. Tuan, H.V. Lai, N.H. Phong, Water pollution estimation based on the 2D transport-diffusion model and the Singular Evolutive Interpolated Kalman filter, C. R. Mecanique 342 (2014) 106–124, https://doi.org/10.1016/j.crme.2013.10.007.
[16] V. Shutyaev, F.-X. Le Dimet, E. Shubina, Sensitivity with respect to observations in variational data assimilation, Russ. J. Numer. Anal. Math. Model. 32 (1) (2017) 61–71, https://doi.org/10.1515/rnam-2017-0006.
[17] L.W. White, B. Vieux, D. Armand, F.-X. LeDimet, Estimation of optimal parameters for a surface hydrology model, Adv. Water Resour. 26 (3) (2003) 337–348, https://doi.org/10.1016/s0309-1708(02)00189-6.
[18] H.S. Hoang, R. Baraille, On the efficient low cost procedure for estimation of high-dimensional prediction error covariance matrices, Automatica 83 (2017) 317–330.